Type Ia Supernova Physics

Wolfgang Eitel Kerzendorf

A thesis submitted for the degree of

Doctor of Philosophy

of The Australian National University

Research School of Astronomy and Astrophysics
The Australian National University
Canberra ACT 0200
Australia

October 2008

Fancy schmancy italic text for a dedication.

Disclaimer

I hereby declare that the work in this thesis is that of the candidate alone, except where indicated below or in the text of the thesis.

Wolfgang E. Kerzendorf

9th May 2011

Acknowledgments

Lorem ipsum dolor sit amet, consectetuer adipiscing elit. Donec tincidunt semper neque. Cum sociis natoque penatibus et magnis dis parturient montes, nascetur ridiculus mus. Donec cursus velit ut felis. Quisque tellus. Curabitur in leo. Suspendisse volutpat. Nunc sodales sagittis magna. In vehicula viverra elit. Donec dapibus cursus mauris. Maecenas volutpat, sapien eu dictum molestie, mi lectus tristique augue, eu lobortis tellus nisi nec urna. Phasellus at est nec odio ultricies consequat. Nam eu urna.

Duis tempus imperdiet nunc. Integer vitae lorem. Sed id pede eu turpis rhoncus semper. Curabitur ante leo, facilisis vitae, interdum mollis, fermentum et, ipsum. Phasellus scelerisque, arcu et varius venenatis, lacus magna semper mauris, et aliquet augue nulla hendrerit libero. Suspendisse nec turpis et nisl congue posuere. Mauris sagittis ipsum nec lectus. Vestibulum nisl. Quisque ante. Nam accumsan, metus eu lobortis laoreet, massa velit elementum urna, ac tristique eros justo sit amet mauris. Vestibulum at arcu hendrerit massa placerat tristique. In magna velit, vestibulum eget, viverra ut, facilisis id, lectus. Cras justo lorem, varius non, tristique sit amet, lobortis nec, neque. Aenean cursus congue metus. Vestibulum id magna.

Abstract

Lorem ipsum dolor sit amet, consectetuer adipiscing elit. Donec tincidunt semper neque. Cum sociis natoque penatibus et magnis dis parturient montes, nascetur ridiculus mus. Donec cursus velit ut felis. Quisque tellus. Curabitur in leo. Suspendisse volutpat. Nunc sodales sagittis magna. In vehicula viverra elit. Donec dapibus cursus mauris. Maecenas volutpat, sapien eu dictum molestie, mi lectus tristique augue, eu lobortis tellus nisi nec urna. Phasellus at est nec odio ultricies consequat. Nam eu urna.

Duis tempus imperdiet nunc. Integer vitae lorem. Sed id pede eu turpis rhoncus semper. Curabitur ante leo, facilisis vitae, interdum mollis, fermentum et, ipsum. Phasellus scelerisque, arcu et varius venenatis, lacus magna semper mauris, et aliquet augue nulla hendrerit libero. Suspendisse nec turpis et nisl congue posuere. Mauris sagittis ipsum nec lectus. Vestibulum nisl. Quisque ante. Nam accumsan, metus eu lobortis laoreet, massa velit elementum urna, ac tristique eros justo sit amet mauris. Vestibulum at arcu hendrerit massa placerat tristique. In magna velit, vestibulum eget, viverra ut, facilisis id, lectus. Cras justo lorem, varius non, tristique sit amet, lobortis nec, neque. Aenean cursus congue metus. Vestibulum id magna.

CONTENTS

LIST OF FIGURES

LIST OF TABLES

CHAPTER 1

INTRODUCTION

For millenia mankind has watched and studied the nightsky. Apart from planets and comets it appeared an immuatble canvas on which the stars rested. It comes as no surprise that for ancient civilizations supernovae (which were very rare events, occuring only every few centuries) were interpreted as important Omens as they broke the paradigm of the unchanging nightskies. As these events are so rare their origin remained a mystery until the middle of the last century Baade & Zwicky (1934) suggested that "the phenomenon of a super-nova represents the transition of an ordinary star into a body of considerably smaller mass". For the last 85 years the "supernova-branch" in astronomy has been developing. There have been many advances, but there are still very unknowns about supernovae. This work addresses two subfields of supernovae: The unsolved progenitor problem for Type Ia Supernovae as well as quantifying the nucleosynthetic yield of Type Ia supernovae from low-resolution spectra.

1.1. Ancient Supernovae

One of the earliest recorded supernovae is SN185. It first appeared in December of 185 and was visible (however fading) till the August of 187. The main record is the *Houhanshu* (Zhao et al., 2006) which had a described it to be close to *α cen*. Follow-up in modern times have revealed a supernova remnant in a distance of roughly 1 kpc near the *α cen* (Zhao et al., 2006). SN185 is often named as the oldest written record of a supernova, this is however sometimes contested as it is still not completely clear if the so called "guest star" was a comet or a supernovae.

The oldest undisputed record of a supernova is SN1006. It was observed worldwide by asian, arabic and european astronomers. mention 1885 in andromedaHartwig (1885)

1.2. Modern supernova observations and surveys

The most famous and often quoted paper is Baade & Zwicky (1934). It termed the term supernova and established the difference between common novae and supernovae. Baade & Zwicky (1934) suggested that these luminous events are caused by the death of stars.

In order to understand the phenomenon of the supernova better Zwicky began a supernova search with the 18-inch Schmidt telescope. He found several supernovae cite?? which in turn inspired Minkowski to classify these supernovae by their spectra Minkowski (1941). He categorized the 14 known objects into two categories. Those without hydrogen he called 'Type I', those with hydrogen he called 'Type II' (see section 1.3 for a more detailed description).

With the advent of affordable computing in the 1960s the first computer controlled telescopes were build. The 24-inch telecope was built by the Northwestern University and was deployed in Corralitos Observatory in New Mexico. This search resulted 14 supernovae.

The 1990's can be described as the decade of the supernova surveys. The Leuschner Observatory Supernova Survey began in 1992 followed shortly by the Berkeley Automatic Imaging Telescope (BAIT). These searches resulted in 15 supernovae by 1994 (van Dyk et al., 1994). One of the most well known discoveries is SN 1994D. This supernovae was observed with the Hubble Space Telescope and resulted in an image that is widely used today (see Figure **??**).

These successful programmes were succeeded by the Lick Observatory Supernova Search (LOSS) using the Katzman Automatic Imaging Telescope (KAIT). By the year 2000 it had found 96 supernovae (Filippenko et al., 2001).

1.3. Supernova classification

Gallia est omnis divisa in partes tres.

The classification of supernovae started in the 1941 when Minkowski realized that there seem to be two main types (Minkowski, 1941). Minkowski relied on optical low-resolution spectra near the maximum to identify the two main subtypes (see Figure **??** for an overview of spectra of different types). Those containing a hydrogen line (6563 Å) he called Type II supernovae and those showing no hydrogen he called Type I supernovae.

This basic classification has remained to this day, however the two main classes branched into several subtypes. During the 1980s the community discovered that most SNe Ia showed a broad Si II line at 6130 Å, but that there was a distinct subclass of objects that lacked this

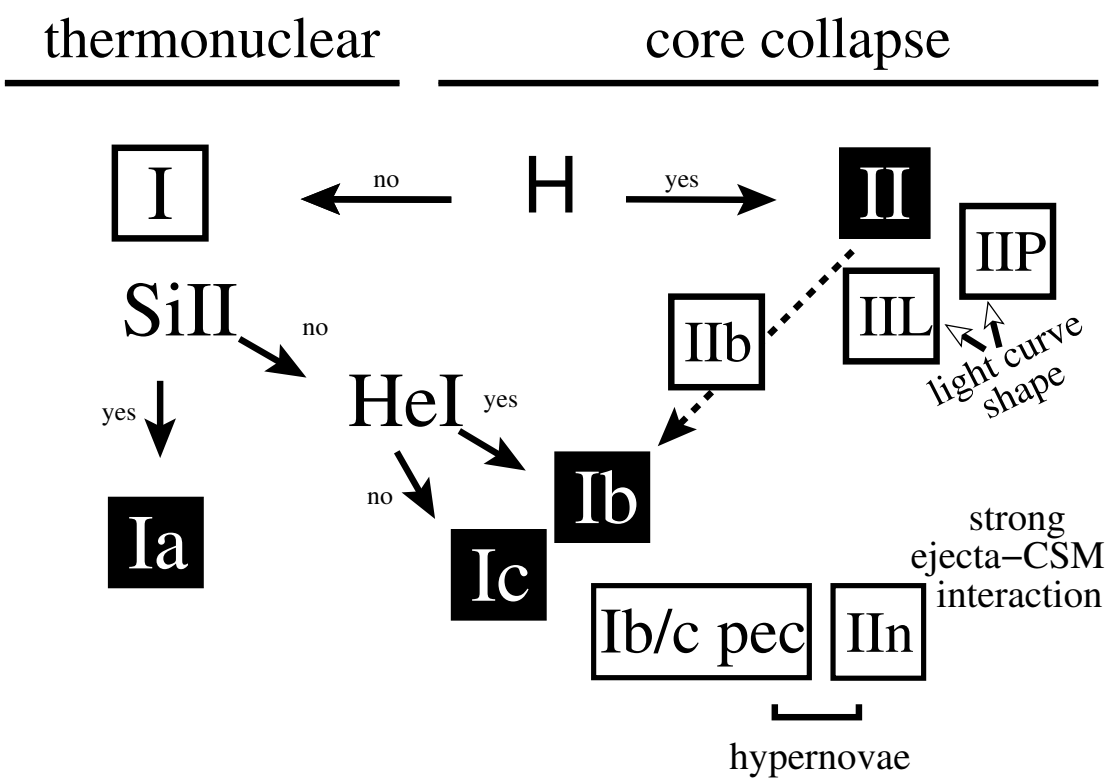

Figure 1.1

feature. These Silicon-less objects were then subclassed further into objects that showed helium – now known as Type Ib – and those that did not were called Type Ic (Harkness et al., 1987; Gaskell et al., 1986). The classical Type I supernova was renamed to Type Ia (see Figure 1.1).

This classification only uses static spectral features. In recent years, however, there has been a push towards also using the lightcurve and spectral evolution as classification parameters. Benetti et al. (2005) provide an overview of this subclassing of SNe Ia and suggest that there are two distinct subclasses of SNe Ia. As a parameter for this further partitioning they use the velocity measured from the Si II feature at 6355 Å. Those with a relatively fast decline in this radial velocity they call HVG (high velocity gradient) those with a slow decline rate are named LVG (low velocity gradient). Figure 1.3 shows the velocity gradient of 26 supernovae taken from Benetti et al. (2005)

Futhermore there seems to be also a split in the intrinsic luminosity of SNe Ia. The canonical objects for these distinct brightness classes are the overluminous 1991T Phillips et al. (1992) and the faint 1991bg . Faint supernovae are fast decliners both in velocity as well as luminosity Benetti et al. (2005). The bright supernovae seem to occur in both the HVG and LVG group. I will discuss the physical implications of these two subtypes in section **??**.

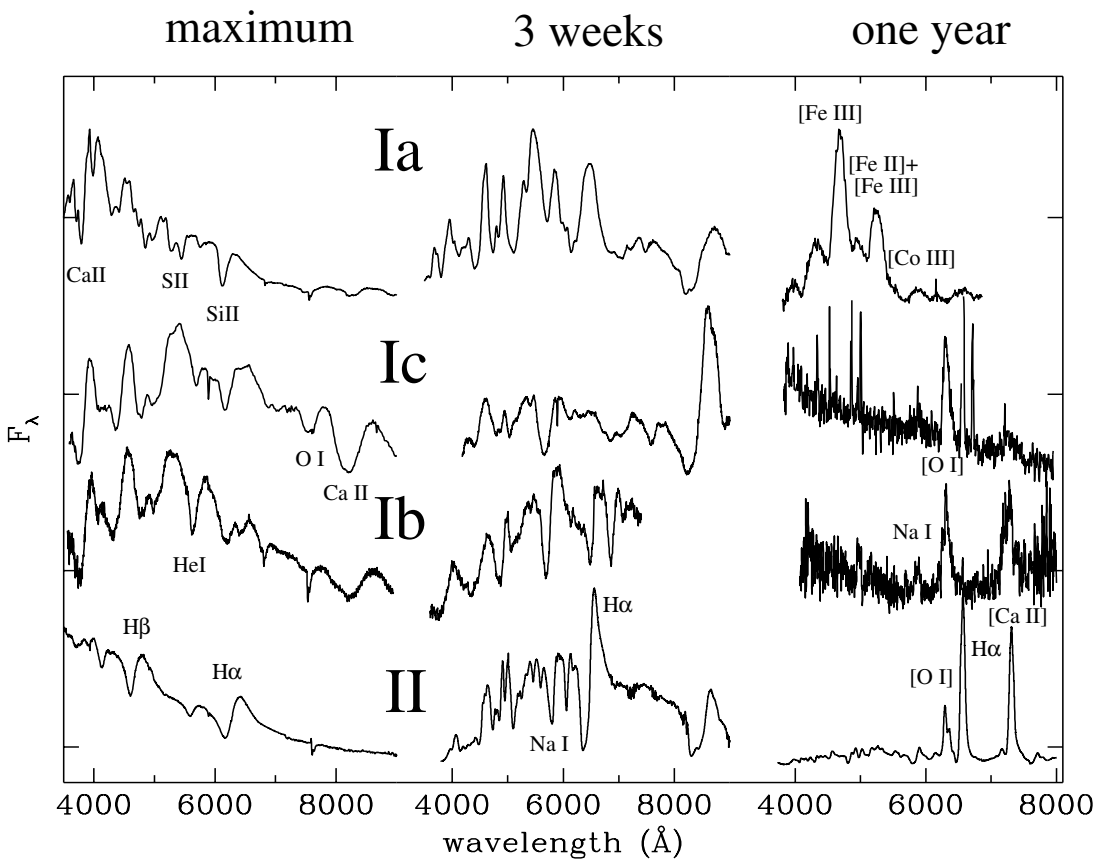

Figure 1.2 example caption

In summary, although there are several different subclasses the SN Iaas a class itself is relatively homogenous when compared to the different SNe II. ??? rates????

SNe IIspan large ranges in observables like luminosity, explosion energies, etc. We can divide the main class into three main subclasses Type II Plateau Barbon et al. (SN IIP 1979) which have a relatively flat light curve after an initial maximum (see Figure **??**), in contrast the Type II Linear (SN IIL Schlegel, 1990) has a rapid linear decline after the maximum. The third subclass is the narrow-lined SN II(SN IIn) which is characterized by narrow emission lines, which are thought to come from interaction with the CSM. Unlike the SNe Iathere are numerous intermediate objects among these three basic classes.

????

For a more comprehensive review of the classification of supernovae the reader should consult Turatto (2003); Turatto et al. (2007).

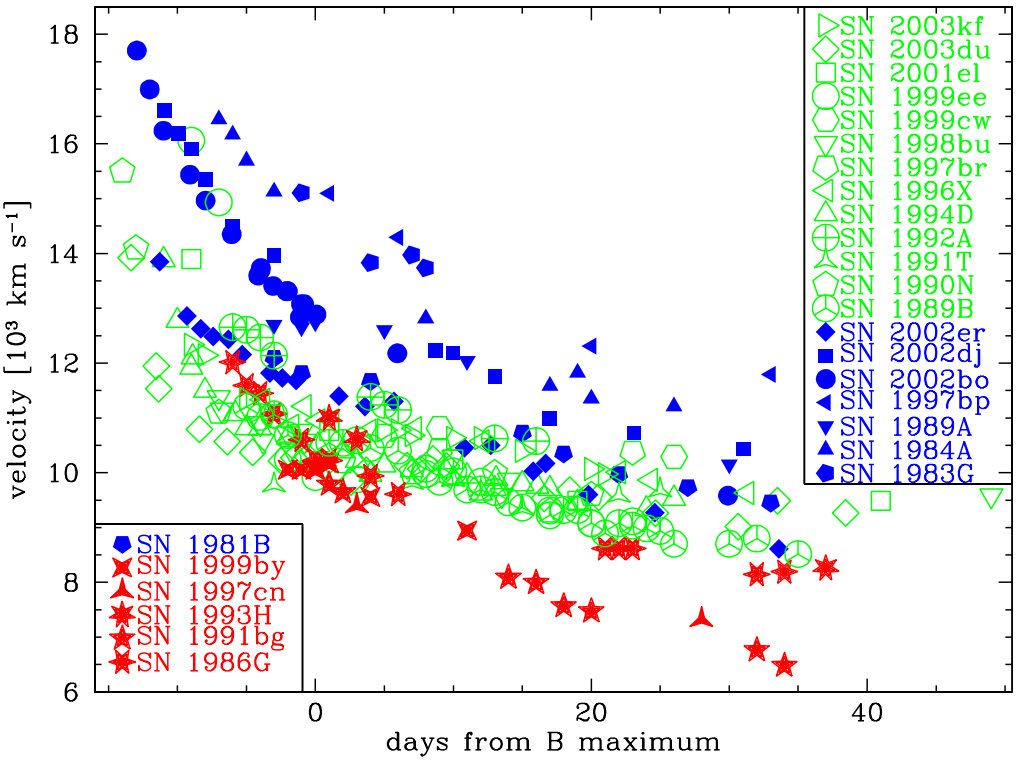

Figure 1.3 example caption

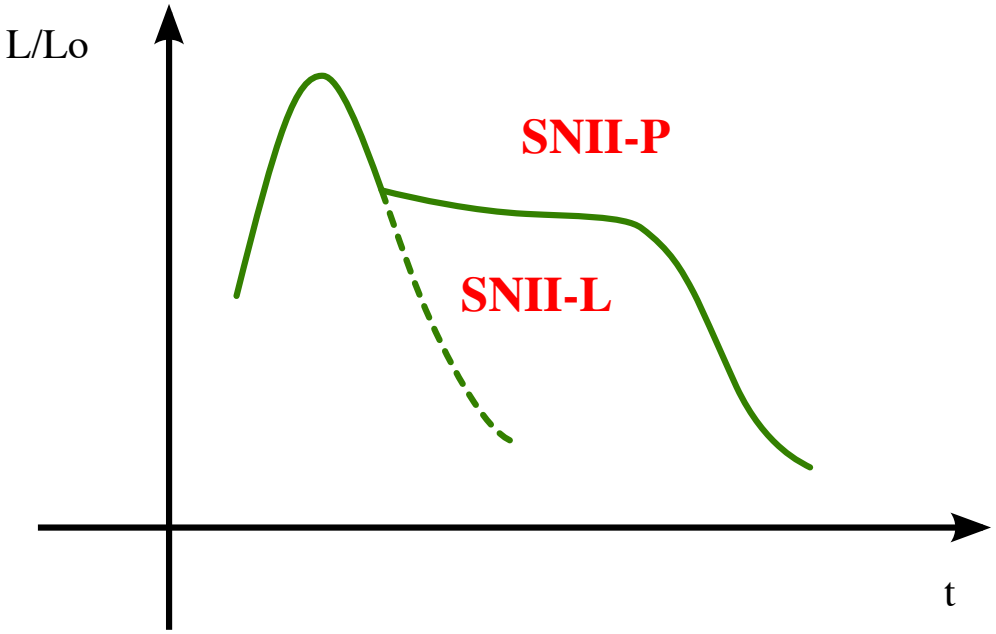

Figure 1.4 example caption

1.4. Core Collapse Supernova

1.4.1. Observation

1.4.2. Theory

All SN IIare believed to be powered by the collapse of the electron-degenerate iron core of massive stars. For the iron core to form there had to be several prior stages of evolution.

Evolution of Massive Stars: To understand the state of the star shortly before supernova evolution it is imperative to follow its evolution. For the topic of SN IIwe will concentrate on the nuclear physics issues of massive star evolution in this section. In the scope of this work we will follow a single massive star as a progenitor. There has been ample of suggestions that SN IIprogenitors are binary, but their evolution is much more complex and is outside the scope of this work?? citation needed??. In this context massive stars are stars bigger than 8 $M_{\odot}$. This is the minimum mass for a star that is believed to explode in a SN II. Like all stars massive stars spend most of their lives on the main-sequence burning hydrogen. This happens via the carbon-nitrogen-oxygen cycle and its various side-channels (e.g $^{12}C(p,\gamma) \rightarrow^{13} N(e^{+}\nu) \rightarrow^{13} C(p,\gamma) \rightarrow^{14} N(p,\gamma)^{15}O(e^{+}\nu) \rightarrow^{15} N(p,\alpha) \rightarrow^{12} C$). For a 20 $M_{\odot}$star this phase lasts for 8.13 Myr(see Woosley et al. (2002)).

As the star evolves it begins to ignite Helium which burns via the triple-α process to Carbon ($3\alpha \rightarrow^{12} C$) and then to Oxygen ($^{12}C(\alpha,\gamma) \rightarrow^{16} O$). Table 1 in Woosley et al. (2002)) lists 1.17 Myr for this phase.

Due to neutrino losses the stellar evolution is qualitatively different after helium burning. A neutrino-mediated Kelvin-Helmholtz contraction of the carbon-oxygen core describes the advanced stages of nuclear burning in massive stars well (Woosley et al. (2002)). This is contraction is occasionally delayed when the burning of new fuel sources counteracts the neutrino losses. The star in the end is composited of a series of shells that burn the above fuel and deposit the ashes on the shell below (see Figure 1.5). There are four distinct burning stages. Their principal fuels are carbon, neon, oxygen, magnesium and silicon.

In the carbon burning stage two ^{12}C nuclei are fused to an excited state

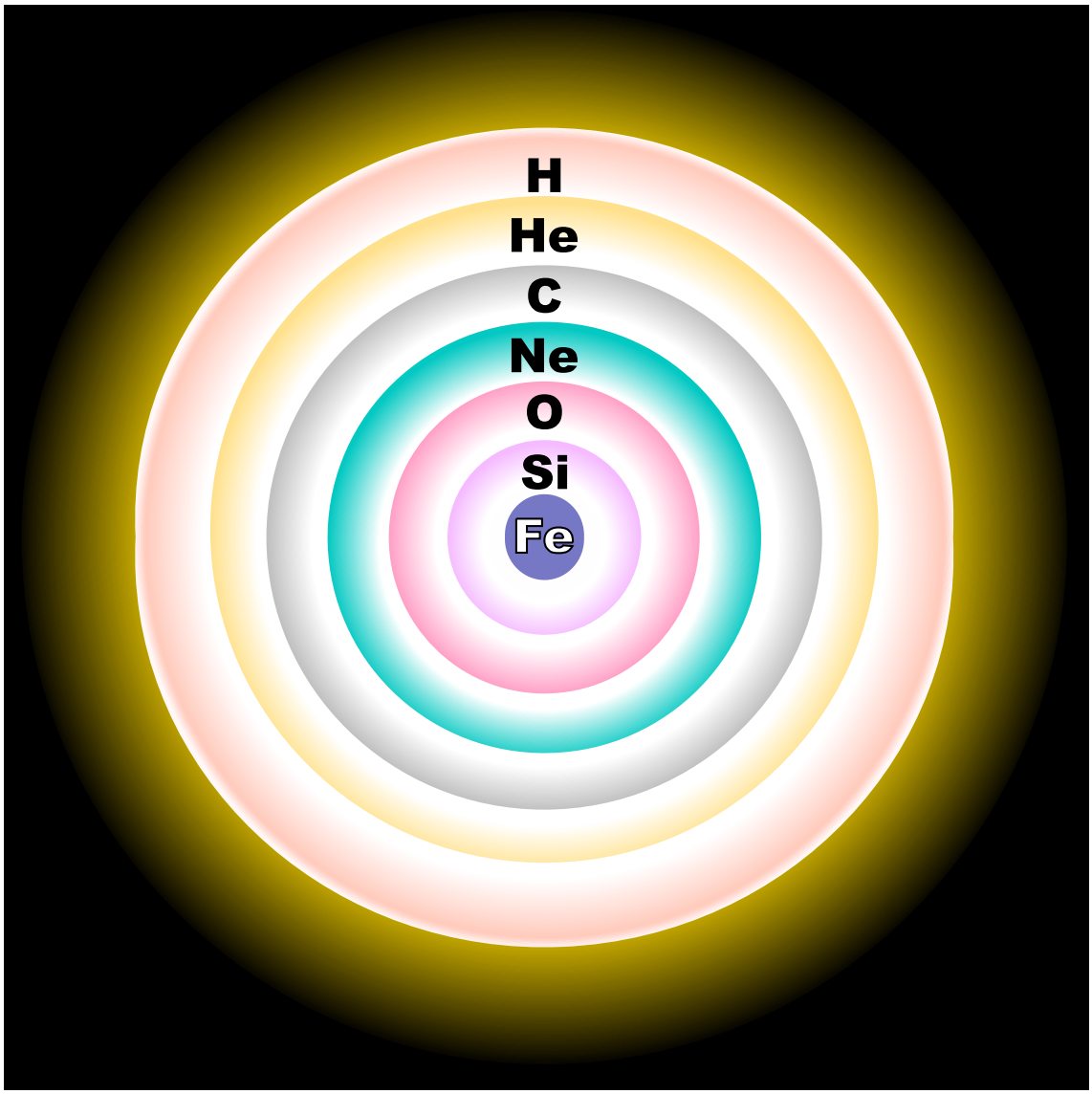

Figure 1.5 example caption

of Magnesium which then decays slowly to ^{23}Na (see 1.2).

$$\begin{aligned} {}^{12}C + {}^{12}C \rightarrow {}^{24}Mg &\rightarrow {}^{23}Mg + n \\ &\rightarrow {}^{20}Ne + \alpha \\ &\rightarrow {}^{23}Na + p \end{aligned} \tag{1.1}$$

Although oxygen has a lower Coulomb barrier, the next nucleus to burn after Carbon is Neon. This layer is composed of of ^{16}O, ^{20}Ne and ^{24}Mg and burns Neon with high-energy photons from the tail of the Planck distribution (^{20}Ne$(\gamma, \alpha)^{16}$O).

Going down one shell, one has now a composition of mainly ^{16}O, ^{24}Mg and ^{28}Si. The bulk nucleosynthetic reaction is shown in **??**.

$$
\begin{aligned}
^{16}C +^{16} O \rightarrow^{28} Si &\rightarrow {}^{31}S + n \\
&\rightarrow {}^{31}P + p \\
&\rightarrow {}^{30}P + d \\
&\rightarrow {}^{28}Si + \alpha
\end{aligned}
\tag{1.2}
$$

The last shell is of burning ^{28}Si to ^{56}Ni is very complex. The obvious reaction ^{28}Si +^{28} Si $\rightarrow^{56}$ Ni does not take place, but is replaced by a very complex network of isotopes to burn to ^{56}Ni. In simulations this is computationally intensive and numerically unstable (e.g . Weaver et al. (1978) who carry a 128-isotope network). Following silicon burning the composition consists of mainly iron-group nuclei. At the end of silicon burning we are reaching nuclear statistical equilibrium.

Core collapse Before the collapse the core, consisting of iron peak elements. Neutrino losses during carbon and oxygen burning decreased the central entropy sufficiently so that the core becomes electron degenerate. Such a degenerate core, which is higher than the Chandrasekhar mass (adjusted for Y_e, entropy, boundary pressure and other parameters will collapse.

There are two main instabilities that facilitate the collapse. AS the density rises the Fermi-Energy becomes high enough for electrons to capture onto iron-group nuclei. This capture process removes electrons that were providing degeneracy pressure and reduces the structural adiabatic index. The second instability is the rise to temperatures where the nuclear statistical equilibrium favours free α-particles. The collapse eventually leads to nuclear densities, the hard-core potential acts as a stiff spring during the compressive phase. It stores up energy and eventually releases this energy. The core bounces. Baron et al. (1985, 1987) believed the core bounce to provide the energy for the ensuing supernova explosion. More recent simulations however show that the bounce shock is not sufficient for a SN IIexplosion. The bounce shock looses energy by photodisintegrating the nuclei it encounters (loosing roughly 10^{51} erg per $0.1\,M_\odot$). Different neutrino flavours that the resulting neutrino winds likely play a big role.

The energy for a successful explosion is now thought to come from neutrino energy deposition. This reinvigorates the shock and leads eventually to an explosion which ejects the envelope of the massive star. A newly born neutron star is left behind.

The precise explosion mechanism is unknown. Using progenitor models with different parameters like rotation and mass lead to different outcomes. Woosley et al. (2002)provide a very comprehensive review of the theory of evolution and core collapse. In particular they lay out a more extensive description of the scenarios after core-bounce.

Pair instability One explosion scenario worth mentioning is that of the pair-instability supernova. This course of events only affects stars with a helium core of more than $40\,M_{\odot}$. After core helium burning the star starts to contract at an accelerated rate. The energy releases during this process is used to produce electron-positron pairs rather than raising the temperature. If significant densities are reached, oxygen fusion eventually halts the implosion and the collapse bounces to an explosion. For very high stellar masses it is believed that oxygen fusion does not provide enough energy to halt the collapse and the star becomes a black hole.

Type II Supernovae The observables of these stellar cataclysm are the light curve, spectra and for one case even the neutrino wind. The supernovae goes through three distinct phases whcih can be observed.

The shock-breakout is the first visible signal from the supernova. Ensman & Burrows (1992) calculated a duration for the shock breakout of SN1987A to 180 s three minutes, its luminosity of $5 \times 10^{44}\mathrm{erg\,s^{-1}}$. Thus far it has been observed only once in 2008D (Soderberg et al., 2008). They report a duration of 400 s with a luminosity of $6.1 \times 10^{43}\mathrm{erg\,s^{-1}}$.

The plateau seen in many SN II(see figure 1.4) is produced by the recombination of hydrogen when hydrogen-rich zones cool to less than 5500 K. The radiation comes effectively from a blackbody, whose luminosity is determined by the radius of the photosphere. Supernovae of Type IIL do not show this behaviour and are thus thought to have no or a very small hydrogen envelope.

After the recombination of hydrogen the light-curve drops off linearly and we see radioactivity providing the main energy source. ^{56}Nidecays to ^{56}Cowith a half-life of 6.1 d and then further to ^{56}Fewith a half-life of 77 d. Most of the energy of the ^{56}Nidecay is used to accelerated the expansion of the core. The tail of the light-curve after the plateau is mainly powered by the decay of ^{56}Co. Some light be also produced by shock interaction with the CSM.

Type Ib/c supernovae If the star lost all of it's hydrogen envelope prior to core-collapse there is no plateau visible in the light-curve. Instead

the light-curve is powered by radio-active decay after shock breakout. In addition, the hydrogen lines are not visible in the spectrum. This leads to the supernova being classified as Type I. If both hydrogen and helium envelopes are lost then the supernova is classified as Type Ic. This loss of envelope is presumed to be caused by stellar winds or binary interactions (citation needed).

1.4.3. Gamma Ray Burst

1.4.4. Type II supernovae as cosmological probes

SN IIPhave been suggested as cosmological probes by Kirshner & Kwan (1974). The importance for cosmological distance probes is that the intrinsic luminosity is known well. Then a simple comparison of apparent magnitude with absolute magnitude results in a distance. At the plateau-phase of the supernova, caused by the hydrogen-recombination, the temperature is well known(T=5000 K). In addition it is assumed that the supernova is in free expansion, thus a measurement of the velocity and an assumption of the initial radius results in a known radius. Assuming the supernova to be a blackbody during plateau-phase one can then calculate a luminosity using the radius and the temperature. SN IIPas distance candles, however, are observationally expensive and not as accurate as SN Iaas standard candels (15% error for SN II(Nugent et al., 2006) vs 7% error for SN Ia).

nucelosynthesis first stars hypernovae GRB connection massive stars expanding photosphere -> distance measurements binary evoltion

1.5. Type Ia Supernova

Although known for a long time, SNe Ia have been prominently featured in astronomy in the last two decades. Their use as standard candles made the measurement of the accelerating universe possible (Riess et al., 1998; Perlmutter et al., 1999)

1.6. Observation

Type Ia Supernova rates The observed supernova frequency carries important information about the underlying progenitor population. The two main suggested progenitors are the single-degenerate system, in which a white dwarf accretes from an non-degenerate companion . The second suggested possibility is the merger of two white dwarfs which results in a SN Ia-explosion (For a more detailed explanation see Section **??**).

Zwicky (1938) was the first work that tried to measure the supernova rate. By monitoring a large number of fields monthly, they arrived at a supernova rate by merely dividing the number of supernova detection by the number of monitoring time and galaxies. This crude method resulted in a rate of one supernova per six centuries.

Over time many improvements were made to this first method. The rate was divided by galaxy morphological class as well as different supernova types. In addition, rates were then defined the supernova rate as number of events per century per $10^{10}\,L_{\odot}$ (e.g. van den Bergh & Tammann, 1991; Tammann et al., 1994). In recent years, however, rate measurements is in relation to star formation rather than photometry (SN per century per $10^{10}\,M_{\odot}$). Therefore the community (e.g. Mannucci et al., 2005) have switched to the use infrared photometry for the galaxy as it is thought to better represent star-formation rate then B-Band photometry (Hirashita et al., 2003).

Figure 1.6 clearly shows that there is a strong connection between morphology and supernova rates. Both progenitor scenarios (single-degenerate and double-degenerate) suggest an "evolved" binary system. It is therefore puzzling that most supernovae occur in late-type spirals with a relative young stellar population. In addition, there is evidence that underluminous SNe Ia (e.g. SN 1991bg) are twice as common in late-type galaxies than in early-type galaxies (Howell, 2001). Furthermore it appears that radio-loud early-type galaxies have an enhanced rate of SNe Iaover radio-quiet galaxies (Della Valle & Panagia, 2003).

All of these factors suggest that SNe Ia can originate from two distinct progenitor scenarios and/or different explosion mechanisms (della Valle & Livio, 1994; Ruiz-Lapuente et al., 1995).

Light curves Light curves are one of the most important observables. The late-time phase gave an important clue to the energy source of the light curve (radioactive decay of ^{56}Ni). In addition, light curves have been successfully used to calibrate SNe Iaas standard candles.

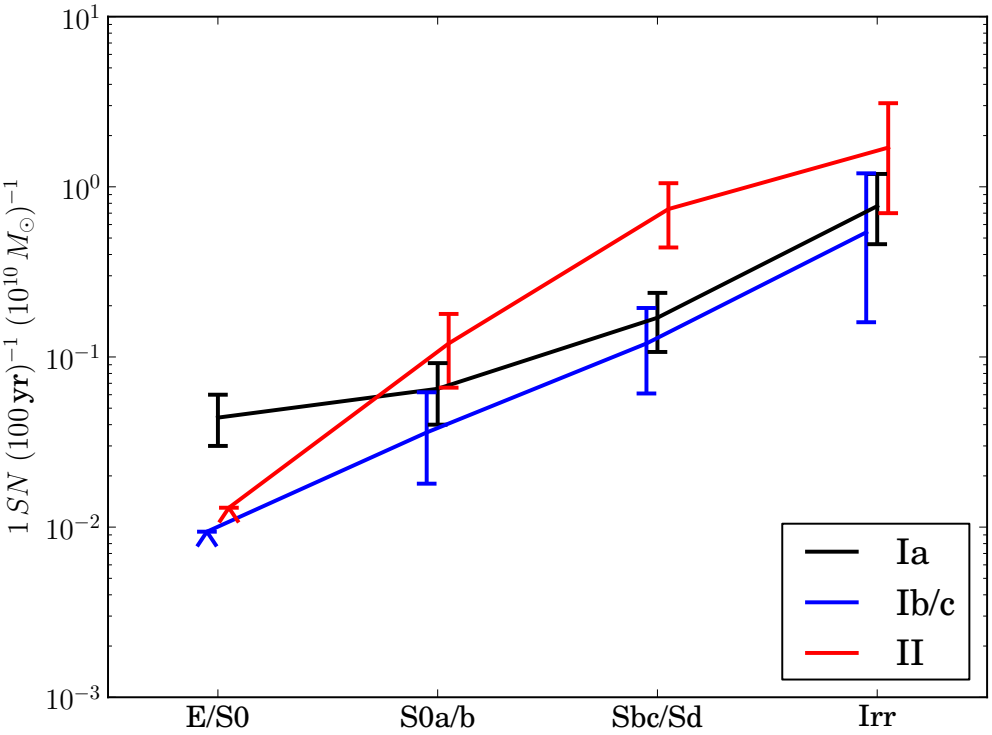

Figure 1.6 example caption

The light curve can be divided in four different phases (see Figure 1.7). In the first phase the SNe Iarises to the maximum brightness. Although only a small fraction of SNe Iahave been observed in that phase. By approximating the very early phase of a SNe Iawith an expanding fireball it is possible to calculate that the rise is 19.5 days (Riess et al., 1999). The luminosity of the fireball is

$$L \propto v^2(t + t_r)^2 T\,,$$

where v is the photospheric velocity, T is the temperature of the fireball, t is the time relative to the maximum and t_r is the rise time.

The rise is very steep and the brightness increases by a factor of ≈ 1.5 per day until 10 days before maximum.

The SN Iareaches the maximum first in the NIRroughly 5 days before the maximum in the B-Band (Meikle, 2000). During the pre-maximum phase the color stays fairly constant at B-V=0.1, but changes non-monotonically to B-V=1.1 30 days after maximum.

The SN Ia starts to fade but a second maximum is observed in the NIR(Wood-Vasey et al., 2008) ??multiple citations. (Kasen, 2006) has

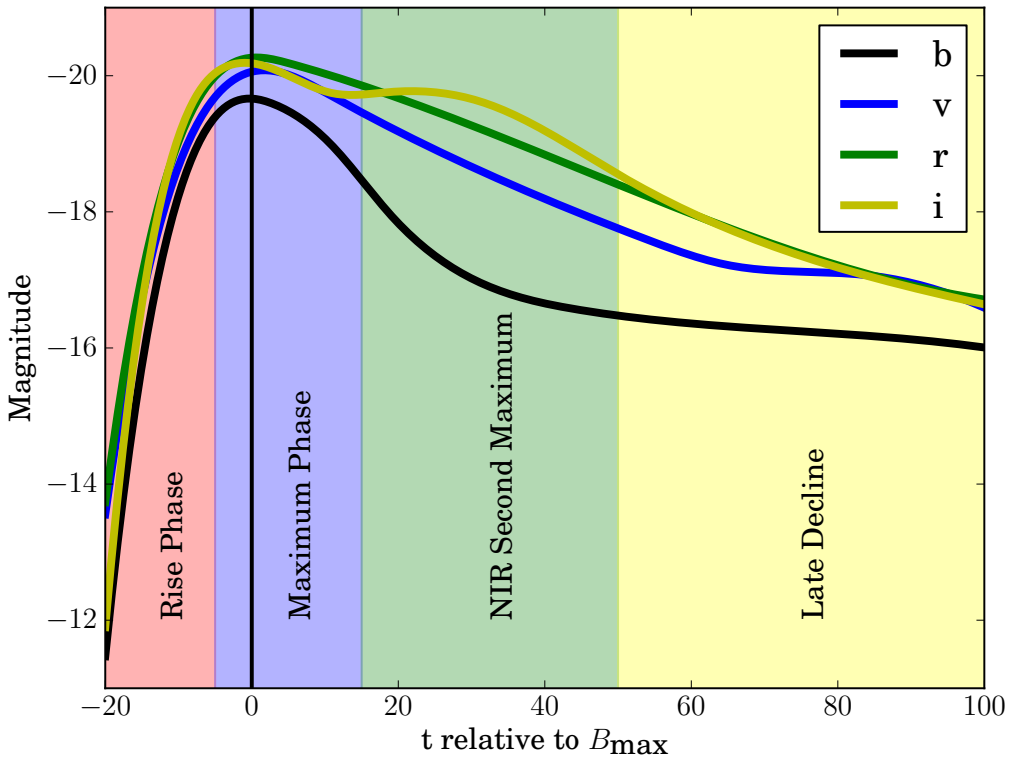

Figure 1.7 example caption

succesfully explained this by fluorescence of iron-peak elements in the NIR. See section **??**.

At roughly 600 days after maximum the light curve begins ???? 1991t had a foreground dust???

Arguably the most important use of light curves is their application in normalizing SNe Ia to standard candles (see Figure **??**). Phillips (1993) plotted the magnitude at maximum in different filters against the decline of the B-Band magnitude after 15 days ($\Delta m_{15}(B)$). They found a strong linear relation with a very high correlation coefficient (> 0.9). Dust extinction in the host is one of the major systematic problems and remains so to this day.

Riess et al. (1995) refined the method by using a linear estimation algorithm. This method would deliver a distance modulus by finding the offset between a template and the supernova lightcurve. They calibrated this method against a set of SNe Ia with known distances. Light curve fitting tools are to this day in active development (e.g. Jha et al., 2007; Guy et al., 2007).

In summary, ... see figure x

Spectra Similar to light curves spectra have different phases. In the pre-maximum phase (tanaka 2010) polarization

X-Ray

Radio

1.6.1. Theory

1.7. Progenitors of Type Ia Supernovae

binary evolution chandrasekhar white dwarfs nucleosynthesis iron in particular

cosmology

1.8. test

CHAPTER 2

SN1572

2.1. Introduction

Type Ia supernovae (SNe Ia) are of broad interest. They serve as physically interesting end points of stellar evolution, are major contributors to galactic chemical evolution, and serve as one of astronomy's most powerful cosmological tools.

It is therefore unfortunate that the identity of the progenitors of SNe Ia is still uncertain. For example, without knowing the progenitors, the time scales of SNe Ia enriching the interstellar medium with iron remains highly uncertain. But it is the crippling impact on the cosmological application of these objects which is especially profound; it is impossible to predict the consequences of any cosmological evolution of these objects or even gauge the likelihood of such evolution occurring.

There is broad agreement that the stars which explode as SNe Ia are white dwarfs which have accreted material in a binary system until they are near the Chandrasekhar mass, then start to ignite carbon explosively, which leads to a thermonuclear detonation/deflagration of the star. It is the identity of the binary companion that is currently completely undetermined. Suggestions fall into two general categories (Iben, 1997):

- Single degenerate systems in which a white dwarf accretes mass from a non-degenerate companion, where the companion could be a main-sequence star, a subgiant, a red giant, or possibly even a subdwarf.
- Double degenerate systems where two CO white dwarfs merge, resulting in a single object with a mass above the Chandrasekhar limit.

The detection of circumstellar material around SN 2006X (Patat et al., 2007) has provided support for the single degenerate model in this case, although the lack of substantial hydrogen in several other SNe Ia (Leonard, 2007) poses more of a challenge to this scenario.

These models also make different predictions for the nature of the system following the explosion. In the double degenerate case, no stellar object remains, but for a single white dwarf, the binary companion remains largely intact.

In the single degenerate case, the expected effect of the SN on the donor star has been investigated by Marietta, Burrows, & Fryxell (2000), who have calculated the impact of a SN Ia explosion on a variety of binary companions. Canal, Méndez, & Ruiz-Lapuente (2001) have explored many of the observational consequences of the possible scenarios, and Podsiadlowski (2003) has presented models that follow both the pre-supernova accretion phase and the post-explosion non-equilibrium evolution of the companion star that has been strongly perturbed by the impact of the supernova shell. To summarize these results, main-sequence and subgiant companions lose 10 – 20 % of their envelopes and have a resulting space velocity of 180 – 320 km s^{-1}. Red-giant companions lose most of its hydrogen envelope, leaving a helium core with a small amount of hydrogen-rich envelope material behind, and acquire a space velocity of about 10 – 100 km s^{-1}. Pakmor et al. (2008) have used a binary stellar evolution code on a main-sequence star and exposed the evolved star to a SN Ia. Their simulations show that even less material is stripped due to the compact nature of a star that evolved in a binary. We will use their results where applicable.

Ruiz-Lapuente et al. (2004, henceforth RP04) have identified what might be the donor star to Tycho's SN, a SN Ia which exploded in the Milky Way in 1572. These authors presented evidence that this star, Tycho-G by their naming convention, is at a distance consistent with the Tycho supernova remnant (henceforth SNR), has a significant peculiar radial velocity and proper motion, roughly solar abundance, and a surface gravity lower than a main-sequence star. However, Tycho-G is located at a significant distance from the inferred center of the remnant, and any process that has displaced the star must preserve the remnant's nearly perfectly circular projected shape. During the final stages of refereeing of this paper we were made aware of the article by Hernandez et al. (2009, henceforth GH09), who used Keck HIRES data to better constrain Tycho-G's stellar parameters, and in addition, found an enhancement in Nickel abundance, relative to normal metal rich stars.

Ihara et al. (2007) have looked for Fe absorption lines from the remnant, using nearby stars as continuum sources, with the hope to better con-

strain the distance of these stars to the SNR. With their technique, stars in the remnant's center should show strong blue-shifted Fe absorption lines, formed by material in the expanding shell of Fe-rich material from the SN, moving towards the observer. Stars in the foreground would show no Fe absorption, and background stars both red- and blue-shifted absorption. Their study shows that Tycho-G does not contain any significant blue-shifted Fe absorption lines, suggesting that Tycho-G is in the remnant's foreground. However, these observations and their analysis, while suggestive, cannot be considered a conclusive rebuttal of Tycho-G's association with the remnant; this technique requires a significant column depth of Fe which is not guaranteed. A lack of Fe column depth may be indicated by the fact that no stars were found in the vicinity of the remnant that showed both blue- and red-shifted absorption lines.

To further examine the RP04 suggested association of Tycho-G with the SN Ia progenitor, we have obtained a high-resolution spectrum of the star using Subaru and its High Dispersion Spectrograph (Noguchi et al., 1998).

We summarize, in section 2, the observational circumstances of the Tycho remnant and any donor star, and argue in section 3 that rapid rotation is an important, previously unrealised signature in a SN Ia donor star. In section 4 we describe our Subaru observations. Section 5 covers the analysis of data and the results of this analysis. Section 6 compares the relative merit for Tycho-G being the donor star to the Tycho SN or being an unrelated background star, and in section 7 we summarize our findings and motivate future observations.

2.2. Observational Characteristics of the Tycho Remnant and Star-G

RP04 have done a thorough job summarizing the relevant details of the Tycho remnant. The remnant shows the characteristics expected of a SN Ia based on its light curve (measured by Tycho Brahe himself), chemical abundances, and current X-ray and radio emission (Ruiz-Lapuente, 2004). In figure 2.1 we have overlaid radio contours[1] on an optical image and have marked the position of the stars mentioned in this and RP04's work.

Although it is not easy to measure the remnant's distance precisely, RP04 estimated Tycho's SNR distance to be 2.8 ± 0.8 kpc, using the ratio

[1]The National Radio Astronomy Observatory is a facility of the National Science Foundation operated under cooperative agreement by Associated Universities, Inc.

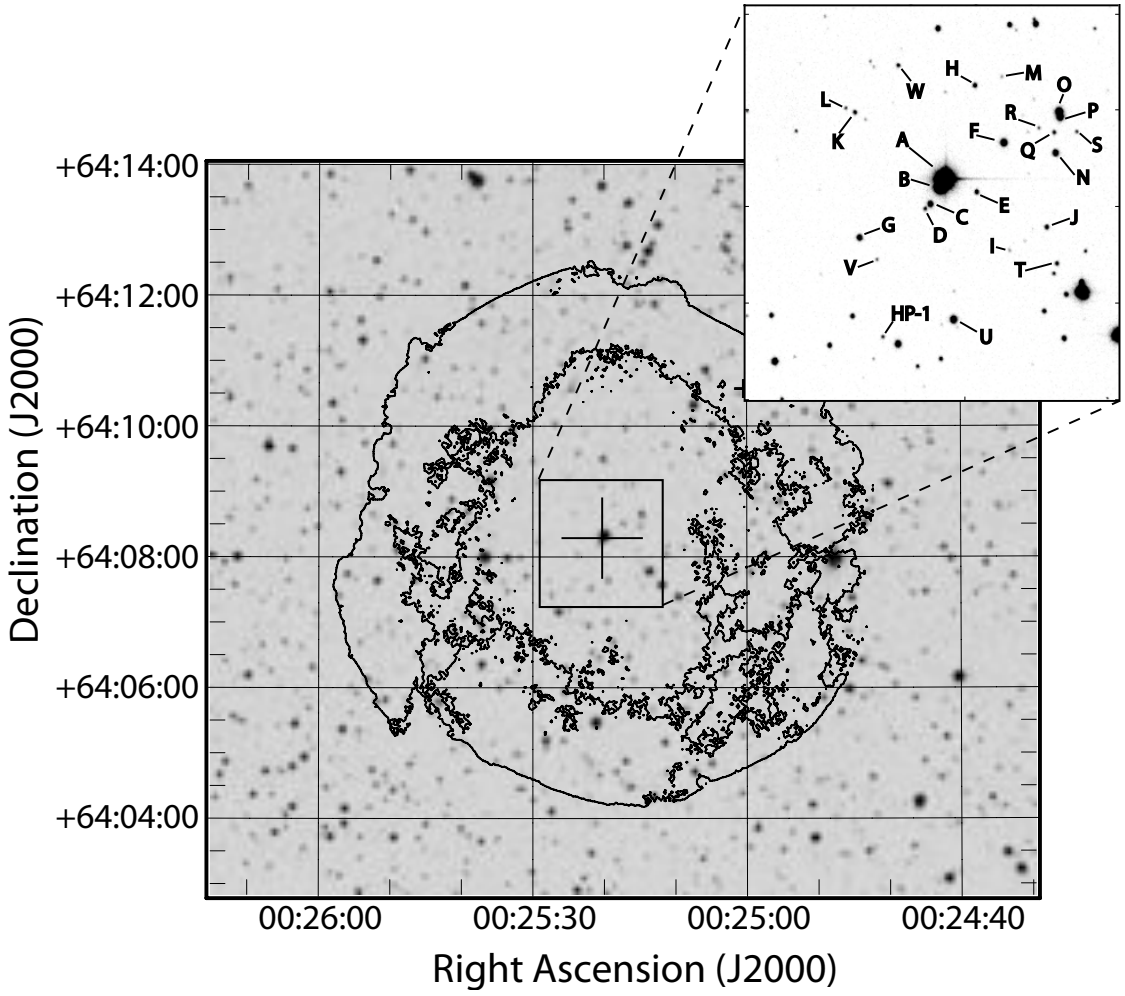

Figure 2.1 Radio Contours (VLA Project AM0347) have been overlaid (Gooch, 1996) on an R-Band Image (NGS-POSS). The cutout is an INT image (see text). The stars marked in the figure are mentioned in this work and in RP04's work.

of the SN 1006 and Tycho SNR's angular sizes and their relative ages, and the direct distance measure of SN 1006 by Winkler, Gupta, & Long (2003). Krause et al. (2008) have recently shown, from a spectrum of a light echo associated with the SN1572, that this SN was a normal SN Ia. Using Tycho's observed light curve, the properties of SN Ia as standard candles, and an extinction value they find a distance to the SN of $3.8^{+1.5}_{-1.1}$ kpc. Updating their values for the extinction values determined in this paper (section 2.6.1), as well as using an absolute magnitude for SN Ia of -19.5 ± 0.25 (Altavilla et al., 2004), we find a distance of $3.4^{+1.3}_{-1.0}$ kpc. In summary, we believe the remnant's distance is poorly constrained, but probably between 2 and 4.5 kpc. RP04 also report the spectroscopic and photometric properties for the bright stars near the center of the Tycho remnant and find a uniform value of approximately $E(B-V) = 0.6$ for stars more distant than 2 kpc. GH09 have revised the

$E(B-V)$ value for Tycho-G to 0.76.

In addition, for a select list of stars, RP04 provide radial velocities and proper motions. For Tycho-G, RP04 report a value of $v_r = -99 \pm 6\,\mathrm{km\ s^{-1}}$ for the radial velocity in the Local Standard of Rest (henceforth LSR), a proper motion of $\mu_b = -6.1 \pm 1.3\,\mathrm{mas\,yr^{-1}}$, $\mu_l = -2.6 \pm 1.3\,\mathrm{mas\,yr^{-1}}$, $\log g = 3.5 \pm 0.5$, and $T = 5750\,\mathrm{K}$. Using HIRES data GH09 have improved the measurements of Tycho-G's stellar parameters, finding $v_r \approx -80\,\mathrm{km\ s^{-1}}$, $\log g = 3.85 \pm 0.3$, $T = 5900 \pm 100\,\mathrm{K}$, and [Fe/H] $= -0.05 \pm 0.09$ dex. We note that Ihara et al. (2007) have classified Tycho-G as an F8V star ($T \approx 6250\,\mathrm{K}$, $\log g \approx 4.3$, Aller et al. 1982), in significant disagreement with the RP04 temperature and gravity. We believe the GH09 values are based on by far the best data, and for the purpose of this paper, we will adopt their values.

Based on the observations, RP04 asserted that Tycho-G was located at approximately $3 \pm 0.5\,\mathrm{kpc}$ – consistent with the remnant's distance. They note that this star has solar metallicity, and therefore its kinematic signature was not attributable to being a member of the Galactic halo. They further argued that Tycho-G's radial velocity and proper motion were both inconsistent with the distance, a simple Galactic rotation model, and the star being part of the disk population of the Milky Way. The derived physical characteristics of the system were nearly identical to what was proposed by Podsiadlowski (2003) for a typical SN Ia donor star emerging from a single degenerate system (e.g., U Sco; also see Hachisu et al., 1996; Li & van den Heuvel, 1997; Hachisu et al., 1999a; Han & Podsiadlowski, 2004; Han, 2008). The revision in the stellar parameters by GH09 leads to different distance with a larger uncertainty, but by and large, has not altered the conclusions above. Taken in total, the data provide a rather convincing case for the association of Tycho-G with the Tycho SN.

2.3. Rapid Rotation: A Key Signature in SN Ia Donor Stars

In the single degenerate SN Ia progenitor channel, mass is transferred at a high rate from a secondary star onto a white dwarf (Nomoto, 1982; Nomoto et al., 2007). These high mass-transfer rates require that the secondary star overflows its Roche lobe. Due to the strong tidal coupling of a Roche-lobe filling donor, the secondary is expected to be tidally locked to the orbit (i.e., have the same rotation period as the orbital period). At the time of the SN explosion, the donor star is released from its orbit, but will continue with the same space velocity as its former

orbital velocity and continue to rotate at its tidally induced rate.

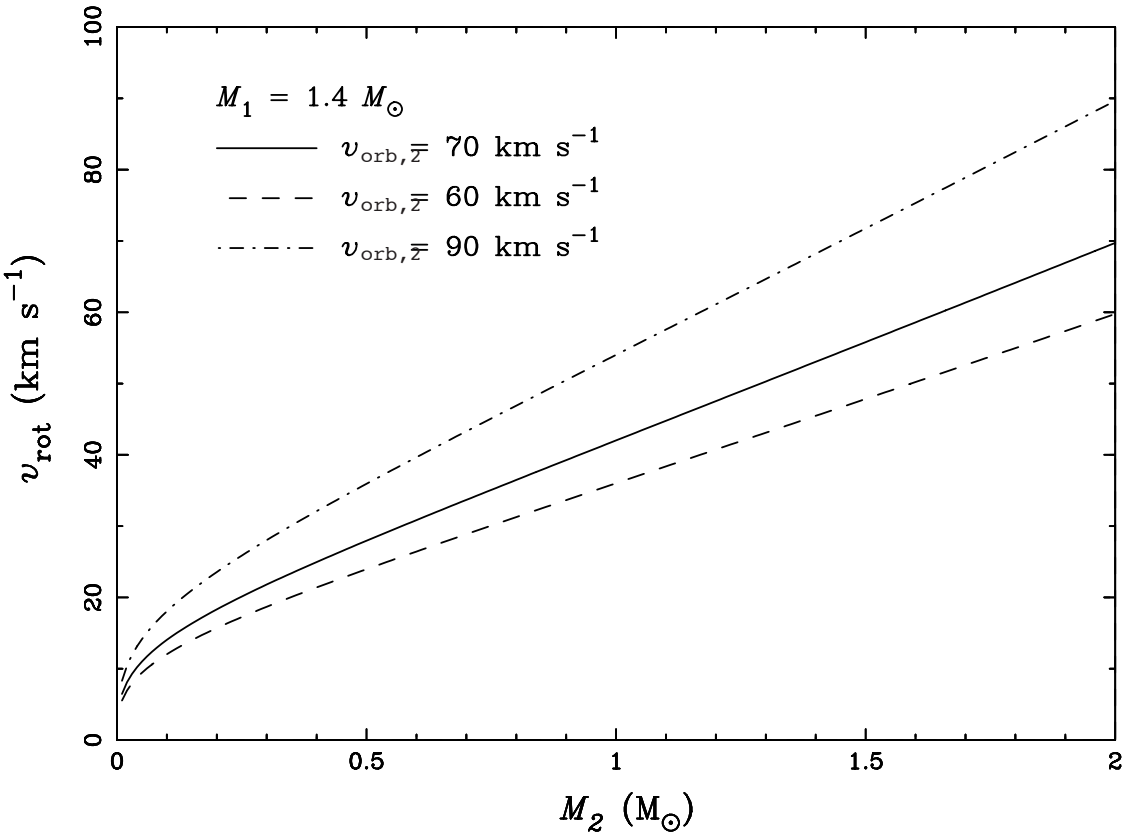

Figure 2.2 The expected rotation rate for a donor star as a function of its mass at the time of the explosion. The three curves show the results for 3 final space velocities of the donor star (similar to those suggested by RP04). It is assumed that the white dwarf has a mass of 1.4 $M_\odot$.

There is a simple relationship between the secondary's rotation velocity ($v_{\mathrm{orb},2}$) and its orbital velocity:

$$v_{\mathrm{rot}} = \frac{M_1 + M_2}{M_1} f(q)\, v_{\mathrm{orb},2},$$

where $f(q)$ is the ratio of the secondary's Roche-lobe radius to the orbital separation (e.g., given by Eggleton, 1983) and $q = M_1/M_2$ is the mass ratio of the components at the time of the explosion. Figure 2.2 shows the rotational velocity as a function of secondary mass for several values of $v_{\mathrm{orb},2}$ (consistent with RP04s measurement, and at the low end of values expected for a subgiant star), where we assumed that the exploding white dwarf had a mass of 1.4 $M_\odot$.

This estimate is strictly speaking an upper limit, as it does not take into account the angular-momentum loss associated with the stripping of envelope material by the supernova and any bloating due to the supernova heating. The latter would reduce the rotational velocity to

first order by a factor equal to the bloating factor (i.e. the ratio of the new to the old radius), but the star would likely find itself in a state where its radius and temperature was atypical of a normal star.

According to the results of Marietta et al. (2000), mass stripping is not likely to be significant if the companion is a main-sequence star or a subgiant. Furthermore, following binary evolution of a main-sequence star, Pakmor et al. (2008) have shown that even less material is stripped. However, if the companion is a giant, it would be stripped of most of its envelope. Such a star would not show any signs of rapid rotation since the initial giant would have been relatively slowly rotating; e.g., if one assumes solid-body rotation in the envelope, the rotation velocity at $\sim 1\,R_\odot$ will only be $\sim 0.5\,\mathrm{km\,s^{-1}}$ for a pre-SN orbital period of 100 d. Moreover, the material at the surface may have expanded from its original radius inside the giant, further reducing the rotational velocity. However, if the stripping is less than estimated by Marietta et al. (2000), then it is possible for the signature of rotation to persist for a giant, albeit at a much lower velocity.

Marietta et al. (2000) also showed that due to the interaction of the SN blast wave with the companion, the secondary may receive a moderate kick of up to a few $10\,\mathrm{km\,s^{-1}}$, but this kick is generally much lower than $v_{\mathrm{orb},2}$ and therefore does not significantly affect the resulting space velocity.

Finally, we note that the observed rotation velocities are reduced by a factor $\sin i$, where i is the inclination angle. However, because the donor star's rotational axis can be assumed to be parallel to its orbital axis, a minimum observed rotation speed can be computed from the observed peculiar radial velocity (observed radial velocity minus the expected radial velocity of an object at that distance and direction). It is only if the orbital motion (and hence final systemic velocity) is solely in the plane of the sky, that $\sin i$, and therefore, the observed rotation, approaches zero.

2.4. Subaru Observations

To investigate the rotational properties of Tycho-G, we were granted time with the Subaru telescope. Our observations of Tycho-G were taken in service mode on the nights of 2005 10 17 and 2005 10 18. 9 spectra were taken with the High Dispersion Spectrograph (HDS, Noguchi et al., 1998) with a resolution of R $\simeq$ 40000 (measured using the instrumental broadening of the Thorium-Argon arc lines), an exposure time of 2000 seconds each (totalling to 5 hours) and a signal to noise ratio of

about 10 per pixel (measured at 8300 Å with 0.1 Å pixel^{-1}) . The HDS features two arms, with each arm feeding a 2-chip CCD mosaic. The blue arm covers 6170 Å to 7402 Å and the red arm 7594 Å to 8818 Å. An OG530 filter was used to block contamination from light blueward of our observing window, and data were binned by 4 in both the spatial and spectral directions, resulting in a pixel size of 0.1 Å (at 8000 Å) by 0.55″.

Data were pre-processed using tools provided by the HDS team and then bias-subtracted. We created a mask from bias and flatfielded frames, where we isolated the echelle orders and flagged bad pixel regions. The data were flatfielded using internal quartz flats, and the 2-D images cleaned of cosmic rays (and checked carefully by eye to ensure there were no unintended consequences) using an algorithm supplied by M. Ashley (private communication). The spectrum of each echelle order was extracted using IRAF[2] echelle routines, with wavelength calibrations based around low-order fits of a Thorium-Argon arc. Wavelength calibration of each extracted spectrum was checked against atmospheric O_2, and our solutions were found to be accurate in all cases to within 1 km s^{-1} (Caccin et al., 1985). Unfortunately, we lacked a smooth spectrum standard star for setting the continuum, and we resorted to calculating a median of the spectra (6 Å window) and dividing the spectra through this smoothed median. This unusual method was chosen over the common approach of fitting the spectrum with a polynomial, due to the special characteristics of this observation (low signal to noise ratio, and a complex instrumental response). While this does not affect the narrow lines our program was targetting, it does affect broad lines such as the Hα and the CaII IR triplet. The final step was to combine all spectra and remove any remaining cosmic rays (in the 1D spectra) by hand.

2.5. Analysis and Results

2.5.1. Rotational measurement

To attain the rotational velocity of the candidate star, we measured several unblended and strong (but not saturated) Fe I lines in the spectrum (Wehrse, 1974). Since our spectrum only had a combined signal to noise ratio of approximately 10, we added the spectra of the lines after

[2]IRAF is distributed by the National Optical Astronomy Observatory, which is operated by the Association of Universities for Research in Astronomy (AURA) under cooperative agreement with the National Science Foundation.

normalizing them to the same equivalent width. As a reference we created three synthetic spectra (one broadened only with the instrumental profile, the others with the instrumental profile and $v_{\rm rot} \sin i$ of 10 and 15 km s^{-1} respectively) with the 2007 version of MOOG (Sneden, 1973), using GH09's temperature, gravity and metallicity. We use a standard value of $\beta = 3/2$ for the limb darkening although the choice of this value is not critical, which we confirmed by checking our results using significantly different values of β. Figure 2.3 shows the comparison between the synthetic spectra of different rotational velocity and the spectrum of Tycho-G. We have scaled the synthetic spectrum using the equivalent width. This comparison indicates that the stellar broadening (rotational, macro turbulence, etc.) is less than broadening due to the instrumental profile of 7.5 km s^{-1}, and therefore we adopt 7.5 km s^{-1} as our upper limit to the rotation of the star. If one were to adopt RP04's measurements of the peculiar spatial motion, it could be concluded that sin i is much closer to 1 than 0 (see the end of section 2.3 for further explanation) and thus that the rotational speed is $v_{\rm rot} \lesssim 7.5$ km s^{-1}.

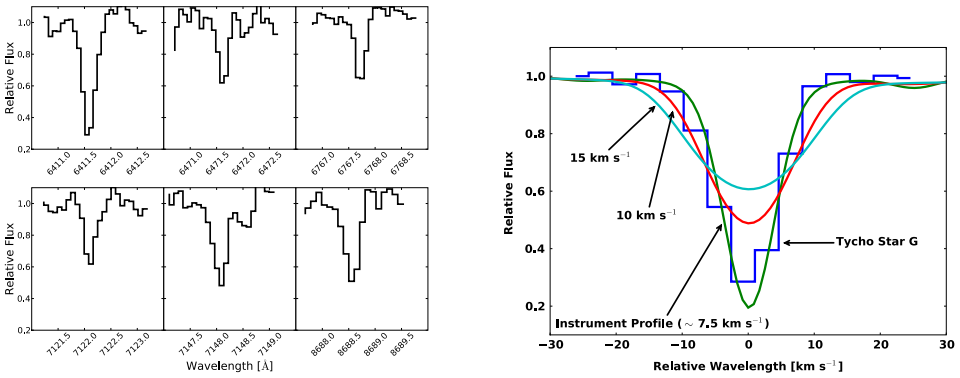

Figure 2.3 Six observed Fe I line profiles of Tycho-G are shown on the left panel. The right panel shows the combination of these line profiles after normalization to the same equivalent width and compares them to the spectrum of the Sun, which is convolved with 3 different values for the rotational broadening kernel. Tycho-G does not show significant rotation, indicating $v_{\rm rot} \sin i \lesssim 7.5$ km s^{-1}.

2.5.2. Radial velocity

To determine the radial velocity, we used 63 lines to measure the shift in wavelength. We find a radial velocity in the topocentric (Mauna Kea) frame of reference of $v_{\rm top} = -92.7 \pm 0.2$ km s^{-1}(the error being the standard deviation of 63 measurements) . The conversion from the topocentric to the Galactic LSR for our observations was calculated to be 13.6 km s^{-1} (IRAF task rvcorrect) using the IAU standard of motion. Including the uncertainty in the LSR definition, we find a radial velocity

in the LSR for Tycho-G of $v_{\rm LSR} = -79 \pm 2\,{\rm km\ s^{-1}}$. This is in significant disagreement with that reported by RP04, but agrees with the revised value published by GH09.

2.5.3. Astrometry

RP04 have measured a significant proper motion for Tycho-G of $\mu_b = -6.1 \pm 1.3\,{\rm mas\,yr^{-1}}$, $\mu_l = -2.6 \pm 1.3\,{\rm mas\,yr^{-1}}$. Because Tycho-G is metal rich, and at a distance of $D > 2$kpc, this measurement provides one of the strongest arguments for Tycho-G being the donor star to Tycho SN. It is almost impossible to account for this proper motion, equivalent to a $v_b = 58\left(\frac{D}{2\ {\rm kpc}}\right)$km s^{-1} or 3 times the disk's velocity dispersion of $\sigma_z =$ 19km s^{-1}, except through some sort of strong binary star interaction.

However, the HST data present an especially difficult set of issues in obtaining astrometry free of systematic errors. For Tycho-G these issues include the PSF on the first epoch WFPC2 image being grossly undersampled, both the ACS and WFPC2 focal planes being highly distorted, poor and different charge transfer efficiency across the two HST images, and that Tycho-G was, unfortunately, located at the edge of one of the WFPC2 chips, making it especially difficult to understand the errors associated with it. Smaller issues include the small field of overlap between the two images, making the measurement subject to issues of the correlated motions of stars, especially in the μ_l direction.

To cross-check RP04's proper motion of Star-G , we have scanned a photographic plate taken in September 1970 on the Palomar 5 meter, and compared this to an Isaac Newton 2.5 m Telescope (INT) CCD archive image (INT200408090414934) of the remnant taken in August 2004. The Palomar plate has an image FWHM of 1.7″, and the INT image 0.88″. While our images have a much larger PSF than the HST images, the images have significantly less distortion, are matched over a larger field of view with more stars, have fully sampled PSFs, and were taken across nearly an 8 times longer time baseline. The photographic nature of the first epoch does add complications not present in the HST data. The non-linear response of photographic plates causes their astrometry to have systematic effects as a function of brightness (Cannon et al., 2001), especially affecting objects near the plate limit, where single grains are largely responsible for the detection of an object.

The position of stars on the INT image were matched to the 2MASS point source catalog (Skrutskie et al., 2006) to get a coordinate transformation (pixel coordinates to celestial coordinates) using a 3rd-order polynomial fit with an RMS precision of 40 mas with 180 stars. This fit is limited by precision of the 2MASS catalog and shows no systematic residuals as a

function of magnitude, or position. Using this world coordinate system (WCS) transformation, we then derived the positions of all stars on the INT image. The coordinates of 60 uncrowded stars on the Palomar plate were matched to the INT-based catalog, and a 3rd-order polynomial was used to transform the Palomar positions to the INT-based positions. The fit has an RMS of 65 mas in the direction of galactic longitude, and 45mas in the direction of galactic latitude. We believe the larger scatter in the direction of Galactic longitude is due to the shape of the PSF being slightly non-symmetric in the direction of tracking on the Palomar plate. This tracking (in RA, which is close to the direction of galactic longitude), causes the position of stars to depend slightly on their brightness. This explanation is supported by a small systematic trend in our astrometric data in μ_l, not seen in μ_b, as a function of m_R. An alternative explanation is that the trend in μ_l is caused by the average motion of stars changing due to galactic rotation as a function of distance, which is proxied by m_R. We have used the Besançon Galactic model (Robin et al., 2003) to estimate the size of any such effect, and find the observed effect is an order of magnitude larger than what is expected. The systemic difference between assuming either source of the observed effect is less than 1 mas yr^{-1} in μ_l, and has no effect in our μ_b measurement. In our final proper motions, presented in table 2.1, we remove the systematic trend as a function of m_R with a linear function.

Table 2.1 Proper motions of stars within 45″ of the Tycho SNR center.

α	δ	μ_l	μ_b	m_R	θ	
[hh:mm:ss.ss]	[dd:mm:ss.ss]	[mas yr^{-1}]	[mas yr^{-1}]	[mag]	[arcsec]	Name
00:25:20.40	+64:08:12.32	-0.90	-0.56	17.05	08.9	c
00:25:18.29	+64:08:16.12	-4.25	-0.81	18.80	10.0	e
00:25:17.10	+64:08:30.99	-1.82	1.78	16.87	20.3	f
00:25:23.58	+64:08:02.02	-1.58	-2.71	17.83	31.1	g
00:25:15.52	+64:08:35.44	1.94	0.83	20.28	31.4	r
00:25:15.08	+64:08:05.95	-0.67	1.49	18.86	33.3	j
00:25:23.89	+64:08:39.33	-0.31	1.08	19.20	33.5	k
00:25:14.74	+64:08:28.16	2.60	1.46	17.45	33.5	n
00:25:14.81	+64:08:34.22	4.05	-2.05	19.35	35.0	q
00:25:13.79	+64:08:34.50	2.32	1.01	19.90	41.3	s
00:25:14.59	+64:07:55.10	-3.94	2.35	19.23	41.7	t
00:25:19.25	+64:07:38.00	1.75	-3.43	16.86	42.1	u
00:25:22.45	+64:07:32.49	81.29	-2.68	19.81	48.7	HP-1

To measure the proper motion of each star, we exclude each star from the astrometric transformation fit so as not to bias its proper motion measurement. Comparing the stellar positions in the 34 year interval

we find that these 60 stars show an RMS dispersion $\sigma_{\mu_l} = 2.1\text{mas yr}^{-1}$, $\sigma_{\mu_b} = 1.6\,\text{mas yr}^{-1}$. For Tycho-G we measure $\mu_l = -1.6 \pm 2.1\,\text{mas yr}^{-1}$, $\mu_b = -2.7 \pm 1.6\,\text{mas yr}^{-1}$; this implies that no significant proper motion is detected. We do note that this measurement has a similar precision to that of RP04, is consistent with no observed motion, and is in moderate disagreement with the RP04 measurement.

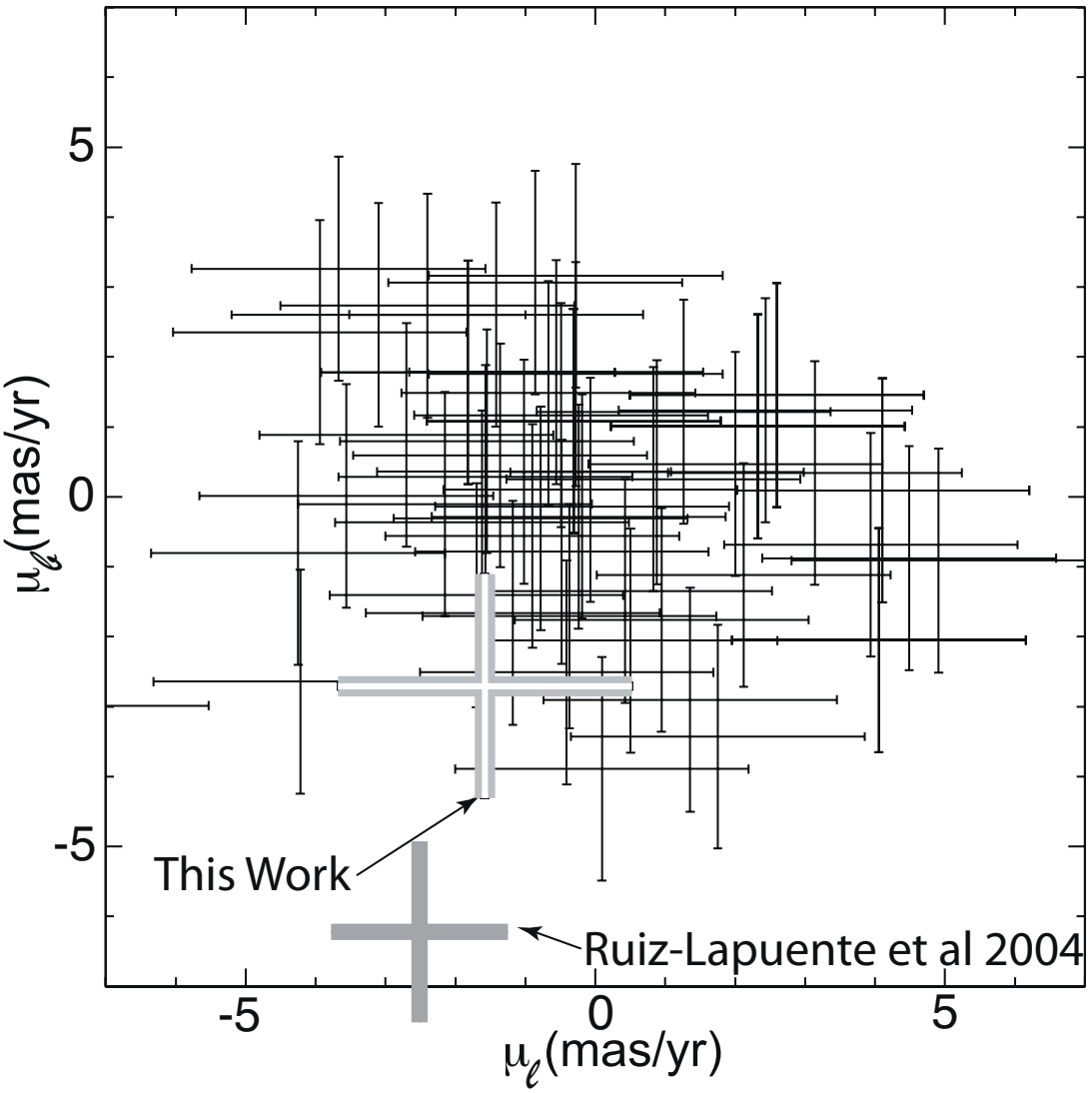

Figure 2.4 The astrometric motions of 60 stars measured in the Tycho SNR center. The measurements have a RMS dispersion of $1.6\,\text{mas yr}^{-1}$. Shown in grey is the proper motion of Tycho-G measured here and by RP04, showing a moderate discrepancy in the two measurements. Our measurement is consistent with no proper motion.

In table 2.1 we present our astrometric measurements of all stars listed by RP04 for which we were able to measure proper motions. We also give the apparent magnitudes in R (partly measured by this work and partly by RP04) and the distance from center θ. Due to crowding caused

by the relatively poor resolution of the first epoch photographic plate, several stars are not included that could be measured using HST. We include an additional star, not cataloged by RP04, which exhibits high proper motion. This high proper motion star, which was off the WFPC2 images of RP04, we designate HP-1, and has a proper motion of μ_l = 81.3, $\mu_b = -2.7$ mas yr^{-1}. Due to the distance from the remnant's center, (we estimate HP-1 would have been located 51'' from the remnant's center in 1572), we doubt this star is connected to the Tycho SN, but we include it for the sake of completeness.

2.6. Discussion

2.6.1. A Background interloper?

A previously unrecognized property for many progenitor scenarios is the rapid post-explosion rotation of the donor (as described in section 2.3). The expected rotation as calculated in Figure 2.2 is large compared to that expected of stars with a spectral type later than F and should be easily observable. We have shown Tycho-G's rotation to be less ($v_{\rm rot} \sin i \lesssim 7.5\,{\rm km\ s^{-1}}$) than what is expected of an associated star if the companion was a main-sequence star or subgiant. A red giant scenario where the envelope's bloating has significantly decreased rotation could be consistent with our observation of Tycho-G, and this will be discussed in section 2.6.2.

The primary basis for which RP04 selected Tycho-G as a candidate for the donor star to the Tycho SN was the combination of its large peculiar radial velocity and its observed proper motion. In Figure 2.5 we use the Besançon Galactic model (Robin et al., 2003) to construct an expected set of radial velocities for metal-rich stars in the direction of SN1572.

Measuring the distance to Tycho-G is a key discriminant in associating the star to the SN explosion. To improve the uncertainty of the distance to the star, due both to temperature and extinction uncertainty, we base our distance on the observed m_K (Skrutskie et al., 2006) and $(V-K)$ color (RP04). We interpolate ATLAS9 models without overshoot (Bessell, Castelli, & Plez, 1998) to find a theoretical $V-K$ and absolute magnitude for the GH09's values of temperature and gravity. Using a standard extinction law (Cardelli, Clayton, & Mathis, 1989) ($A_V = 3.12E(B-V)$ and $A_K/A_V = 0.109$) to match the theoretical and observed colors, we find $A_V = 2.58\pm0.08$mag, $A_K = 0.28\pm0.01$ mag, and $E(B-V) = 0.84\pm0.05$. To better show the uncertainties, we present our distance moduli scaled to the observed and derived values of extinction, temperature and gravity. The temperature coefficients were determined by integrating

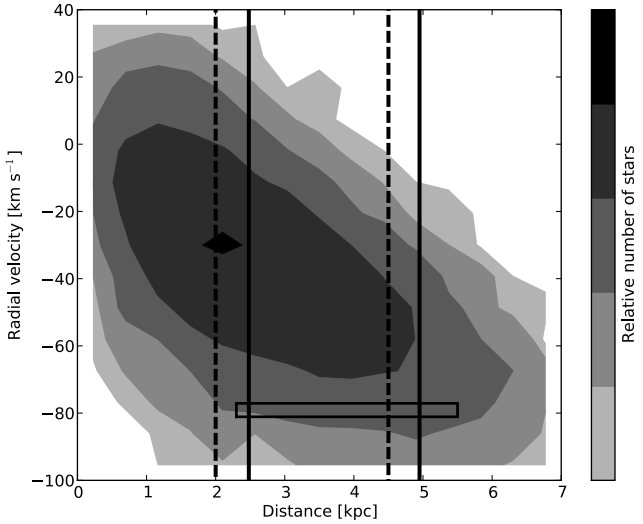

Figure 2.5 Besançon model for a metal rich ([Fe/H] > -0.2) Galactic population between 0 and 7 kpc in the direction of Tycho SNR (l = 120.1, b=1.4) with a solid angle of 1 square degree. The remnant's distance is represented by the black dashed lines (as calculated in section 2.2). The contours show the radial velocity distribution. Our measured radial velocity corrected to LSR and our distance are shown, with their respective error ranges, as the black rectangle. The distance range calculated by GH09 are indicated by the two solid lines. The observed LSR v_r for Tycho-G is mildly unusual for stars at the remnant's distance, and is consistent with the bulk of stars behind the remnant.

blackbodies of the appropriate temperature with a filter bandpass and fitting a powerlaw to the resulting flux.

$$(m_V - M_V) = 12.93 - 3.12(E(B-V) - 0.84) - 2.5(\log g - 3.85) + \quad (2.1)$$
$$+2.5\log\left(\frac{M}{1\,M_\odot}\right) + 2.5\log\left(\frac{T_{\rm eff}}{5900}\right)^{4.688}$$
$$(m_K - M_K) = 12.93 - 0.275(E(B-V) - 0.84) - 2.5(\log g - 3.85) + \quad (2.2)$$
$$+2.5\log\left(\frac{M}{1\,M_\odot}\right) + 2.5\log\left(\frac{T_{\rm eff}}{5900}\right)^{1.937}$$

Assuming a companion mass of $1\,M_\odot$ we find a $(m - M) = 12.93 \pm 0.75$ mag. This uncertainty is dominated by the precision of $\log g$, and equates to a distance of $D = 3.9 \pm 1.6$kpc. Tycho-G, within the errors, is at a distance consistent with the remnant. As seen in Figure 2.5, the observed radial velocity of Tycho-G is consistent with a significant fraction of stars in its allowed distance range. We also note that if Tycho-G is indeed associated with the SN, that it is likely that Tycho-G could have a mass considerably less than $1\,M_\odot$, due to mass transfer and subsequent interaction with the SN, although in this case, the distance to the star would still be consistent with SNR distance.

Ihara et al. (2007) looked for absorption due to Fe I in the remnant's expanding ejecta for 17 stars within the Tycho remnant. No such absorption was seen in the spectrum of Tycho-G, potentially placing it in front of the remnant. However, the amount of Fe I currently within the remnant is uncertain with predicted column densities spanning several orders of magnitude ($0.02 - 8.9 \times 10^{15}\,\mathrm{cm}^{-2}$; Hamilton & Fesen, 1988; Ozaki & Shigeyama, 2006). Therefore, we do not believe the lack of significant Fe I 3720 absorption in Tycho-G to be significant.

In summary, we find that Tycho-G's radial velocity, distance, and stellar parameters are all consistent with an unrelated star, but also with it being the donor star. There is disagreement in Tycho-G's measured proper motion. The measurements of RP04 are inconsistent with normal disk stars at the known distance and strongly point to Tycho-G being associated with the SN, whereas the measurements presented here are consistent with a normal disk star, unrelated to the SN. In addition, we have shown the rotation of Tycho-G is low (confirmed by GH09; $v_{\mathrm{rot}} \leq 6.6\,\mathrm{km\ s}^{-1}$), arguing against association with the SN, as does its off center placement in the remnant. Finally, GH09 have presented evidence that Tycho-G is strongly enhanced in Nickel, an observation that, if confirmed, would strongly point to an association of the star with the SN. If either the high proper motion, or significant Nickel enhancement can be confirmed, then it is likely that Tycho-G is the SN donor star. Otherwise, we believe it is much more likely that Tycho-G is simply an interloper.

2.6.2. Tycho-G as the Donor Star to the Tycho SN

While the case for Tycho-G's association with the SN is not conclusive, it is intriguing, and we believe it is worthwhile to look for a consistent solution assuming the association is true. While not apriori probable, a self-consistent model can be constructed in which Tycho-G was the companion, as we shall discuss now.

To make such a model work, Tycho-G has to be a stripped giant that presently mimics a G2IV star. At the time of the explosion, the star would have been a moderately evolved giant (in a binary with an orbital period $\sim 100\,\mathrm{d}$). The SN ejecta will strip such a giant of almost all of its envelope (Marietta et al., 2000) due to its low binding energy; only the most tightly bound envelope material outside the core will remain bound. Due to the heating by the SN, even this small amount of material (perhaps a few $\times 0.01\,M_{\odot}$) will expand to giant dimensions, and the immediate-post-SN companion will have the appearance of a luminous red giant. However, because of the low envelope mass, the thermal

timescale of the envelope is sufficiently short that it can loose most of its excess thermal energy in 400 years and now have the appearance of a G2IV star (Podsiadlowski, 2003).

A lower mass for Tycho-G ($0.3 - 0.5\,M_{\odot}$) also reduces the distance estimate, and makes the observed radial velocity more unusual for stars at this distance. The expected spatial velocity depends on the pre-SN orbital period and should be in the range of $30 - 70\,\mathrm{km\,s^{-1}}$ for a period range of $20 - 200\,\mathrm{d}$ (Justham et al., 2008). These velocities are consistent with the inferred spatial velocity of the object relative to the LSR if Tycho-G is at the distance of the remnant, even if no significant proper motion has been measured (see Figure 2.5).

A stripped-giant companion would link the progenitor to the symbiotic single-degenerate channel (Hachisu et al., 1999b) for which the symbiotic binaries TCrB and RS Oph are well studied candidates. Indeed, (Justham et al., 2008) argued that the ultracool low-mass helium white dwarfs (with masses $> 0.3\,M_{\odot}$) that have been identified in recent years are most likely the stripped-giant companions that survived SN Ia explosions, which could provide some further possible support for such a scenario for Tycho-G.

If the association is real, Tycho-G's displacement to the SE of the geometric center of the remnant as defined by radio and X-ray observations might be interpreted as being due to the remnant's interaction with an inhomogeneous ISM. Deep optical images of the remnant do show extended diffuse emission along the eastern and northeastern limbs interpreted as shock precursor emission (Ghavamian et al., 2000). This along with an absence of detected Balmer-dominated optical emission along the whole of the western and southern limbs suggests a density gradient of the local interstellar medium with increasing density towards the NE. An east-west density gradient has also been inferred from detailed radio expansion rate measurements (Reynoso et al., 1997). Such an E–W density gradient could have led to a more rapid expansion toward the west giving rise to a small shift in the apparent geometric center away from the SE without creating a highly distorted remnant. However, there are problems with this explanation. Deviations from spherical symmetry in both radio and X-ray images of the remnant are relatively small (Reynoso et al., 1997; Cassam-Chenaï et al., 2007), and the remnant is most extended along the eastern and northeastern limbs, just where one finds the greatest amount of extended diffuse optical emission. Moreover, the remnant's expansion rate appears lowest toward the northeast (PA = 70 degrees), not the southeast (Reynoso et al., 1997). Although the argument that Tycho-G's SE displacement from the remnant's current geometric center is a result of an asymmetrical expansion is not strong, it remains a possibility.

The most conclusive way of confirming a stripped-giant scenario for Tycho-G would be an independent, precise measurement of the distance to Tycho-G which in combination with measurements of the gravity and effective temperature would help to constrain Tycho-G's mass. Unfortunately, such a measurement will most likely have to wait for the advent of the GAIA satellite. Alternatively, one may be able to single out a stripped giant from a normal G2IV star through nucleosynthesis signatures, specifically evidence for CNO-processed material (or other nucleosynthetic anomalies). While a normal G2IV star is unlikely to show CNO-processed material at the surface, a stripped giant is likely to do so. Unfortunately, the data presented here are not of adequate quality to explore the detailed properties of Tycho-G's atmosphere.

2.7. Outlook and Future Observations

Presently, we believe the evidence for Tycho-G's association with the Tycho SN is interesting, but not conclusive. A possible scenario if Tycho-G is the donor star, would be that of a stripped giant scenario discussed in section 6. However, there are still other stars that have not been adequately scrutinized. Ihara et al. (2007) have found a star (RP04 Star-E) which may contain blueshifted Fe I lines, indicating their association with the remnant. Unfortunately, the star has neither a significant peculiar radial velocity (Ihara et al. 2007; RP04) nor a significant peculiar proper motion (RP04 and confirmed by our work; see Table 2.1).

High-resolution spectroscopy of each candidate in the remnant's center is necessary to precisely determine each star's physical parameters. However, the small observed velocities of the remaining stars suggest that the donor star would have needed to be a giant at the time of explosion. Using RP04's observed values, none of the stars in the remnant's center appear consistent with what is expected of a giant star as the donor star except possibly for Star-A. We also note that there is an additional star present in archived HST images, not cataloged in RP04, offset from RP04's star A by 0.5″ E and 0.2″ N at $m_V = 16.8$, $(B - V) = 1.0$. This star, near the remnant's centre, has a color consistent with an F-star (assuming that it is behind the bulk of the line of sight reddening), but it will require adaptive optics to obtain its spectrum given its proximity to the 13th magnitude Star-A. This star could potentially be a non-giant progenitor.

If future observations are unable to pinpoint a viable donor star, other progenitor scenarios will have to be considered. These include the double degenerate scenario, or a scenario where there is a long time

delay between the accretion phase of a donor star onto the white dwarf, and the ultimate supernova explosion.

We would like to thank the Subaru HDS team for taking these observations in service mode. This paper makes use of data obtained from the Isaac Newton Group Archive which is maintained as part of the CASU Astronomical Data Centre at the Institute of Astronomy, Cambridge. This publication makes use of data products from the Two Micron All Sky Survey, which is a joint project of the University of Massachusetts and the Infrared Processing and Analysis Center/California Institute of Technology, funded by the National Aeronautics and Space Administration and the National Science Foundation. This work also makes use of POSS-I data. The National Geographic Society - Palomar Observatory Sky Atlas (POSS-I) was made by the California Institute of Technology with grants from the National Geographic Society. WEK, BPS and MA are supported by the Australian Research Council (grant numbers DP0559024, FF0561481). This paper was conceived as part of the Tokyo Think Tank collaboration, and was supported in part by the National Science Foundation under Grant No. PHY05-51164. This work was supported in part by World Premier International Research Center Initiative (WPI Program), MEXT, Japan, and by the Grant-in-Aid for Scientific Research of the Japan Society for the Promotion of Science (18104003, 18540231, 20540226) and MEXT (19047004, 20040004). Additionaly we would like to thank Pilar Ruiz Lapuente and her team for the valuable discussions we had in regards to the manuscript. We would also like to thank our referee, who provided us with a very detailed and thorough analysis of the first manuscript and subsequent revisions.

CHAPTER 3

SN1006

Lorem ipsum dolor sit amet, consectetuer adipiscing elit. Mauris posuere, elit ac suscipit pulvinar, purus felis vehicula purus, sed pellentesque arcu nibh eu turpis. Vivamus volutpat convallis mi. Aliquam varius magna eu urna lacinia dignissim. Proin venenatis tellus. Fusce pede dui, semper varius, venenatis vitae, ultrices ac, dolor. Proin diam. Suspendisse eget purus id leo accumsan scelerisque. Integer rutrum. Etiam risus nibh, auctor eu, eleifend id, interdum ut, odio. Suspendisse potenti. Praesent ultricies, mauris convallis vestibulum viverra, nulla risus porttitor tellus, ut consequat velit nunc at nisi. Nulla rhoncus nisl quis urna. Morbi sed nunc at tortor rhoncus iaculis. Lorem ipsum dolor sit amet, consectetuer adipiscing elit. Sed augue. Nunc molestie.

Maecenas at lectus id nunc bibendum placerat. Suspendisse cursus, magna vitae blandit bibendum, nisi justo facilisis mi, at faucibus elit urna id felis. Lorem ipsum dolor sit amet, consectetuer adipiscing elit. Maecenas risus erat, ornare ac, varius nec, molestie sed, nulla. Praesent sem urna, sollicitudin in, vulputate at, suscipit vehicula, lectus. Integer mollis. Curabitur ornare, erat a facilisis sagittis, risus nulla faucibus diam, at vehicula justo magna nec urna. Pellentesque rhoncus, turpis eu facilisis molestie, diam ipsum tristique massa, nec auctor risus diam quis metus. Lorem ipsum dolor sit amet, consectetuer adipiscing elit. Fusce varius iaculis neque. Aliquam erat volutpat. Cras sit amet nisi sit amet diam imperdiet molestie. Quisque nec nisl. Cras nisi velit, pharetra sed, cursus nec, euismod ac, turpis.

Morbi tincidunt, tellus nec dignissim congue, risus libero sollicitudin tellus, sit amet porta magna libero sed ante. In id orci eget nibh ultrices ultrices. Sed feugiat lobortis augue. Integer

nulla. Phasellus lacus diam, ornare id, ornare ut, dictum non, velit. Ut egestas, risus quis placerat fringilla, nisl nunc tincidunt ligula, et blandit dui diam vel sem. Morbi mattis turpis et purus pellentesque accumsan. Mauris enim massa, sollicitudin at, lobortis quis, ultricies sed, nunc. Pellentesque habitant morbi tristique senectus et netus et malesuada fames ac turpis egestas. In in arcu. Vestibulum ante ipsum primis in faucibus orci luctus et ultrices posuere cubilia Curae; Donec eleifend molestie enim. Etiam justo. Sed pharetra ultrices lectus. Mauris imperdiet varius purus. Aliquam commodo adipiscing est. Pellentesque vitae odio fringilla pede viverra tempor. Vivamus sed sem. Quisque molestie elementum lorem. Proin aliquam odio vel sapien.

Quisque urna. Praesent scelerisque tortor nec elit. Pellentesque non urna. Duis non sapien id nunc rutrum facilisis. Donec lectus ipsum, ullamcorper vel, sollicitudin a, tempor a, sapien. Nam dui. In hac habitasse platea dictumst. Integer eu ligula id lacus sollicitudin sodales. Nam aliquam nibh vitae urna gravida rutrum. Aliquam erat volutpat. Integer gravida mattis tellus. Etiam ipsum lacus, dapibus id, volutpat eget, vestibulum vel, pede. In odio quam, viverra id, adipiscing nec, consequat ut, orci. Nunc sit amet neque eu risus dictum ultrices. Proin sem quam, ullamcorper ut, posuere at, tempus eget, nibh. Cras ipsum. Phasellus bibendum purus eu enim. In hac habitasse platea dictumst. Praesent eget leo ac sem congue sodales.

Nunc malesuada turpis vitae neque. Donec sollicitudin libero vel nisi. Aliquam congue sem sed est. Integer eget ipsum. Nam eu mauris. Aliquam vehicula tempor nulla. Duis faucibus ornare elit. Vivamus nunc. Phasellus placerat, orci non blandit scelerisque, neque urna faucibus justo, non gravida pede sem a urna. Sed eget arcu eget enim pellentesque tincidunt. Cum sociis natoque penatibus et magnis dis parturient montes, nascetur ridiculus mus. In in nulla sed est venenatis sagittis. Mauris nibh orci, adipiscing in, blandit quis, vulputate vitae, tortor. Quisque venenatis. Ut leo quam, pellentesque vitae, dictum ut, vestibulum at, turpis. Aliquam id urna. Vestibulum nunc mauris, facilisis sed, molestie quis, consequat non, dui.

Duis id metus et tortor viverra varius. Vivamus consequat. Sed bibendum ultricies lectus. Pellentesque vulputate orci vitae augue. Vivamus dignissim pharetra mauris. Lorem ipsum dolor sit amet, consectetuer adipiscing elit. Vestibulum purus purus, commodo in, consequat eu, lobortis eu, sem. Proin volutpat, pede eu imperdiet bibendum, nulla odio lobortis eros, eu aliquet neque nunc eu enim. Donec non nunc. Aliquam erat volutpat. Ut cursus

fermentum orci.

Class aptent taciti sociosqu ad litora torquent per conubia nostra, per inceptos himenaeos. Donec ante eros, porttitor vel, pellentesque sit amet, laoreet ut, velit. Vestibulum sit amet turpis sed lorem vestibulum vulputate. Maecenas sed orci in ante pharetra accumsan. Sed id nibh. Pellentesque dapibus varius neque. Pellentesque habitant morbi tristique senectus et netus et malesuada fames ac turpis egestas. Nullam ultrices augue. Lorem ipsum dolor sit amet, consectetuer adipiscing elit. Etiam convallis placerat tortor. Suspendisse potenti. Mauris porttitor, justo et mollis dapibus, dui nunc accumsan dolor, quis sollicitudin est nisi at libero. Donec sollicitudin eros sed neque. Nunc at quam.

Donec id arcu. Sed vel sapien sit amet metus vestibulum fringilla. Etiam fringilla ligula at arcu. Donec bibendum sem et quam. Nam diam mauris, malesuada vel, placerat a, fermentum sit amet, lectus. Cras venenatis justo nec leo. Aliquam vulputate erat. Cras turpis. Cras gravida. Aliquam erat volutpat. Sed porta pretium ligula. Mauris viverra, nisi euismod vulputate lobortis, est tortor consectetuer arcu, at congue quam ipsum sit amet sem. Cum sociis natoque penatibus et magnis dis parturient montes, nascetur ridiculus mus. Mauris eget dolor.

Suspendisse pulvinar. Suspendisse felis nisl, mattis sed, facilisis at, laoreet vitae, magna. Suspendisse potenti. Pellentesque et ligula vel mauris suscipit vestibulum. Phasellus eros sem, volutpat at, feugiat ut, aliquam sed, augue. In hac habitasse platea dictumst. Suspendisse suscipit. Cum sociis natoque penatibus et magnis dis parturient montes, nascetur ridiculus mus. In lectus dolor, commodo non, ultricies eu, scelerisque at, orci. Nulla semper. Suspendisse potenti. Donec orci diam, pellentesque tristique, tempus eget, tincidunt in, dolor. Maecenas tristique vehicula risus. Integer vitae nisi. Aenean sed enim eu nisl suscipit scelerisque. Integer non metus. Donec dui erat, bibendum eu, suscipit eu, facilisis non, erat. Morbi dapibus pede id justo. Fusce lobortis volutpat enim.

Morbi leo turpis, facilisis in, ultrices vel, adipiscing ut, erat. Praesent ligula. Maecenas quis velit in orci adipiscing aliquam. Quisque at pede. Integer at odio. Pellentesque feugiat tellus sed risus. Mauris et turpis. Nam sodales. Suspendisse mollis tincidunt sapien. In ac sapien et purus sollicitudin ultricies. Integer eget sapien quis ligula commodo egestas. Nulla aliquam, odio sed tincidunt blandit, pede dolor gravida nunc, nec condimentum lorem nulla eget dui.

BIBLIOGRAPHY

Aller, L. H. et al. 1982, Landolt-Börnstein: Numerical Data and Functional Relationships in Science and Technology (Berlin: Springer)

Altavilla, G. et al. 2004, MNRAS, 349, 1344

Baade, W., & Zwicky, F. 1934, Proceedings of the National Academy of Science, 20, 254

Barbon, R., Ciatti, F., & Rosino, L. 1979, A&A, 72, 287

Baron, E., Bethe, H. A., Brown, G. E., Cooperstein, J., & Kahana, S. 1987, Physical Review Letters, 59, 736

Baron, E., Cooperstein, J., & Kahana, S. 1985, Physical Review Letters, 55, 126

Benetti, S. et al. 2005, ApJ, 623, 1011, arXiv:astro-ph/0411059

Bessell, M. S., Castelli, F., & Plez, B. 1998, A&A, 333, 231

Caccin, B., Cavallini, F., Ceppatelli, G., Righini, A., & Sambuco, A. M. 1985, A&A, 149, 357

Canal, R., Méndez, J., & Ruiz-Lapuente, P. 2001, ApJ, 550, L53

Cannon, R., Hambly, N., & Zacharias, N. 2001, in Astronomical Society of the Pacific Conference Series, Vol. 232, The New Era of Wide Field Astronomy, ed. R. Clowes, A. Adamson, & G. Bromage, 311–+

Cardelli, J. A., Clayton, G. C., & Mathis, J. S. 1989, ApJ, 345, 245

Cassam-Chenaï, G., Hughes, J. P., Ballet, J., & Decourchelle, A. 2007, ApJ, 665, 315

della Valle, M., & Livio, M. 1994, ApJ, 423, L31

Della Valle, M., & Panagia, N. 2003, ApJ, 587, L71, arXiv:astro-ph/0303255

Eggleton, P. P. 1983, ApJ, 268, 368

Ensman, L., & Burrows, A. 1992, ApJ, 393, 742

Filippenko, A. V., Li, W. D., Treffers, R. R., & Modjaz, M. 2001, in Astronomical Society of the Pacific Conference Series, Vol. 246, IAU Colloq. 183: Small Telescope Astronomy on Global Scales, ed. B. Paczynski, W.-P. Chen, & C. Lemme, 121–+

Gaskell, C. M., Cappellaro, E., Dinerstein, H. L., Garnett, D. R., Harkness, R. P., & Wheeler, J. C. 1986, ApJ, 306, L77

Ghavamian, P., Raymond, J., Hartigan, P., & Blair, W. P. 2000, ApJ, 535, 266

Gooch, R. 1996, in Astronomical Society of the Pacific Conference Series, Vol. 101, Astronomical Data Analysis Software and Systems V, ed. G. H. Jacoby & J. Barnes, 80–+

Guy, J. et al. 2007, A&A, 466, 11, arXiv:astro-ph/0701828

Hachisu, I., Kato, M., & Nomoto, K. 1996, ApJ, 470, L97

Hachisu, I., Kato, M., & Nomoto, K. 1999b, ApJ, 522, 487

Hachisu, I., Kato, M., Nomoto, K., & Umeda, H. 1999a, ApJ, 519, 314

Hamilton, A. J. S., & Fesen, R. A. 1988, ApJ, 327, 178

Han, Z. 2008, astro-ph/08031986, accepted for publication in ApJL

Han, Z., & Podsiadlowski, P. 2004, MNRAS, 350, 1301

Harkness, R. P. et al. 1987, ApJ, 317, 355

Hartwig, E. 1885, Astronomische Nachrichten, 112, 360

Hernandez, J. I. G., Ruiz-Lapuente, P., Filippenko, A. V., Foley, R. J., Gal-Yam, A., & Simon, J. D. 2009, ApJ, 691, 1

Hirashita, H., Buat, V., & Inoue, A. K. 2003, A&A, 410, 83, arXiv:astro-ph/0308531

Howell, D. A. 2001, ApJ, 554, L193, arXiv:astro-ph/0105246

Iben, I. J. 1997, in NATO ASIC Proc. 486: Thermonuclear Supernovae, ed. P. Ruiz-Lapuente, R. Canal, & J. Isern (Dordrecht: Kluwer), 111

Ihara, Y., Ozaki, J., Doi, M., Shigeyama, T., Kashikawa, N., Komiyama, K., & Hattori, T. 2007, PASJ, 59, 811

Jha, S., Riess, A. G., & Kirshner, R. P. 2007, ApJ, 659, 122, arXiv:astro-ph/0612666

Justham, S., Wolf, C., Podsiadlowski, P., & Han, Z. 2008, submitted

Kasen, D. 2006, ApJ, 649, 939, arXiv:astro-ph/0606449

Kirshner, R. P., & Kwan, J. 1974, ApJ, 193, 27

Krause, O., Tanaka, M., Usuda, T., Hattori, T., Goto, M., Birkmann, S., & Nomoto, K. 2008, Nature, 456, 617

Leonard, D. C. 2007, ApJ, 670, 1275

Li, X.-D., & van den Heuvel, E. P. J. 1997, A&A, 322, L9

Mannucci, F., Della Valle, M., Panagia, N., Cappellaro, E., Cresci, G., Maiolino, R., Petrosian, A., & Turatto, M. 2005, A&A, 433, 807, arXiv:astro-ph/0411450

Marietta, E., Burrows, A., & Fryxell, B. 2000, ApJS, 128, 615

Meikle, W. P. S. 2000, MNRAS, 314, 782, arXiv:astro-ph/9912123

Minkowski, R. 1941, PASP, 53, 224

Noguchi, K., Ando, H., Izumiura, H., Kawanomoto, S., Tanaka, W., & Aoki, W. 1998, in Proc. SPIE, Optical Astronomical Instrumentation, ed. S. D'Odorico, Vol. 3355, 354

Nomoto, K. 1982, ApJ, 253, 798

Nomoto, K., Saio, H., Kato, M., & Hachisu, I. 2007, ApJ, 663, 1269

Nugent, P. et al. 2006, ApJ, 645, 841, arXiv:astro-ph/0603535

Ozaki, J., & Shigeyama, T. 2006, ApJ, 644, 954

Pakmor, R., Röpke, F. K., Weiss, A., & Hillebrandt, W. 2008, A&A, 489, 943, 0807.3331

Patat, F. et al. 2007, Science, 317, 924

Perlmutter, S. et al. 1999, ApJ, 517, 565, arXiv:astro-ph/9812133

Phillips, M. M. 1993, ApJ, 413, L105

Phillips, M. M., Wells, L. A., Suntzeff, N. B., Hamuy, M., Leibundgut, B., Kirshner, R. P., & Foltz, C. B. 1992, AJ, 103, 1632

Podsiadlowski, P. 2003, astro-ph/0303660

Reynoso, E. M., Moffett, D. A., Goss, W. M., Dubner, G. M., Dickel, J. R., Reynolds, S. P., & Giacani, E. B. 1997, ApJ, 491, 816

Riess, A. G. et al. 1998, AJ, 116, 1009, arXiv:astro-ph/9805201

——. 1999, AJ, 118, 2675, arXiv:astro-ph/9907037

Riess, A. G., Press, W. H., & Kirshner, R. P. 1995, ApJ, 438, L17, arXiv:astro-ph/9410054

Robin, A. C., Reylé, C., Derrière, S., & Picaud, S. 2003, A&A, 409, 523

Ruiz-Lapuente, P. 2004, ApJ, 612, 357

Ruiz-Lapuente, P., Burkert, A., & Canal, R. 1995, ApJ, 447, L69+, arXiv:astro-ph/9505090

Ruiz-Lapuente, P. et al. 2004, Nature, 431, 1069

Schlegel, E. M. 1990, MNRAS, 244, 269

Skrutskie, M. F. et al. 2006, ApJ, 131, 1163

Sneden, C. 1973, ApJ, 184, 839

Soderberg, A. M. et al. 2008, Nature, 453, 469, 0802.1712

Tammann, G. A., Loeffler, W., & Schroeder, A. 1994, ApJS, 92, 487

Turatto, M. 2003, in Lecture Notes in Physics, Berlin Springer Verlag, Vol. 598, Supernovae and Gamma-Ray Bursters, ed. K. Weiler, 21–36, arXiv:astro-ph/0301107

Turatto, M., Benetti, S., & Pastorello, A. 2007, in American Institute of Physics Conference Series, Vol. 937, Supernova 1987A: 20 Years After: Supernovae and Gamma-Ray Bursters, ed. S. Immler, K. Weiler, & R. McCray, 187–197, 0706.1086

van den Bergh, S., & Tammann, G. A. 1991, ARA&A, 29, 363

van Dyk, S. D., Treffers, R. R., Richmond, M. W., Filippenko, A. V., & Paik, Y. 1994, in Bulletin of the American Astronomical Society, Vol. 26, American Astronomical Society Meeting Abstracts, 1444–+

Weaver, T. A., Zimmerman, G. B., & Woosley, S. E. 1978, ApJ, 225, 1021

Wehrse, R. 1974, A list of all Fraunhofer lines of the Rowland tables arranged by elements (Heidelberg: Universität)

Winkler, P. F., Gupta, G., & Long, K. S. 2003, ApJ, 585, 324

Wood-Vasey, W. M. et al. 2008, ApJ, 689, 377, 0711.2068

Woosley, S. E., Heger, A., & Weaver, T. A. 2002, Reviews of Modern Physics, 74, 1015

Zhao, F., Strom, R. G., & Jiang, S. 2006, Chinese J. Astron. Astrophys., 6, 635

Zwicky, F. 1938, ApJ, 88, 529

Appendices

Long Boring Tables